

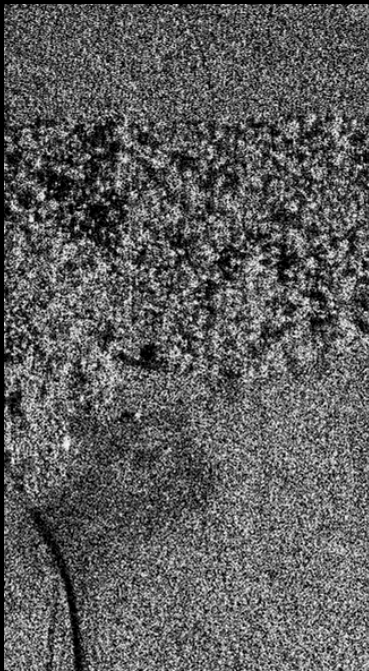
Ground Moving Target Indication (GMTI) with Synthetic Aperture Radar (SAR)



Nick Marechal
The Aerospace Corp.
February 6, 2012

Aerospace Staff Signal Processing Contributions

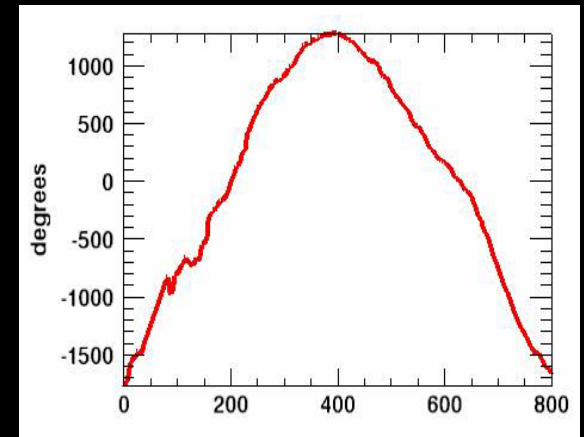
- Richard Dickinson
- Grant Karamyan



One of eight image channels



Mover revealed in
Clutter Suppressed Imagery



Mover phase as a function
of slow time

Ground Moving Targets in SAR Imagery

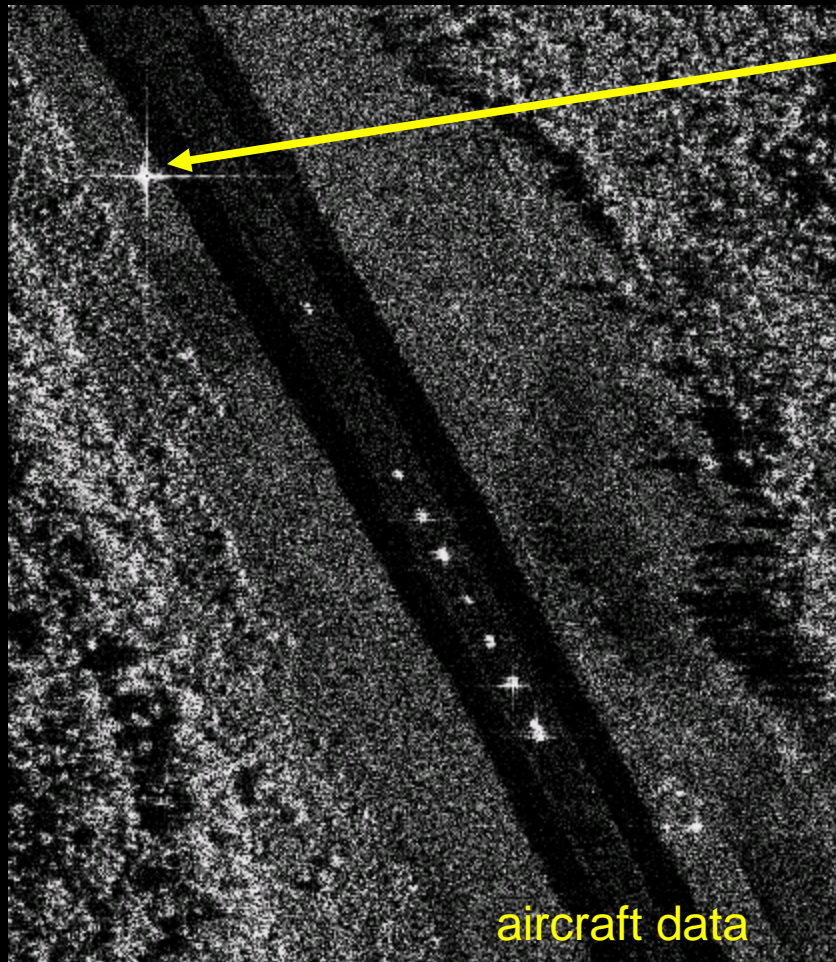
Outline

- Nominal Moving Target Phase Equations
- Measured Moving Target Phase Examples
- Space Time Adaptive Processing (STAP) Review
- STAP applied to 8 channel SAR image data (element space, phase centers)
 - Single 3 sec coherent integration full azimuth resolution
 - Ten 0.3 second coherent integration times, results in SAR movie of moving vehicle

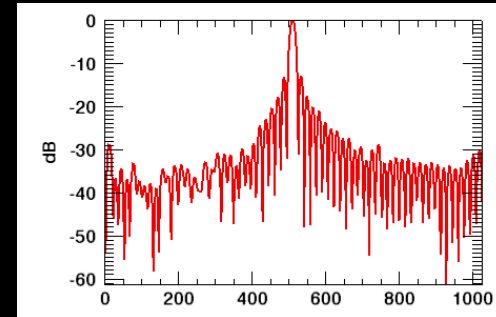
Airborne X-band Image Example

Azimuth Impulse Response (IPR) and Residual Phase Error Shown

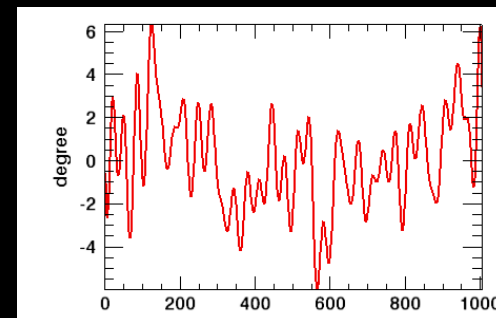
- Image of corner reflector (single look)



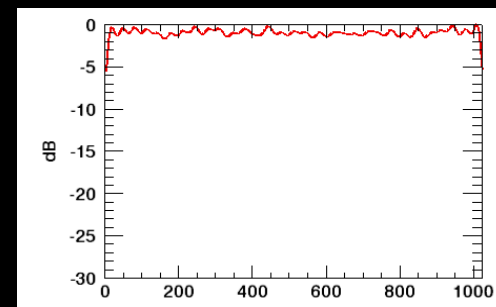
Corner Reflector
Azimuth-Doppler IPR



Corner Reflector
Azimuth Phase
(unwrap phase of FFT
of IPR)



Corner Reflector
Azimuth-Amplitude
(amp of FFT of IPR)



Ground Moving Target Indication (GMTI)

Moving Point Target Phase Characteristics

Go To Paper on Moving Target Phase



Quadratic Phase & Nonzero Doppler Rate

- Quadratic phase defocuses Doppler/azimuth IPR
- Formula for quadratic expressed for polar format processed data
- Target energy can be focused by phase compensation
- Stationary Targets do not exhibit 1000's deg of phase

Note: CDP = 2.71 sec.

Quadratic Phase (polar format processing)

$$Q = 90 \left(\frac{\mathbf{v} \cdot \mathbf{u}_y T}{\Delta y} + \frac{\mathbf{a} \cdot \mathbf{u}_x T^2}{\lambda} \right) \text{ (degrees)}$$

\mathbf{v} = target velocity vector

\mathbf{a} = target acceleration vector

\mathbf{u}_x = slant plane range unit vector

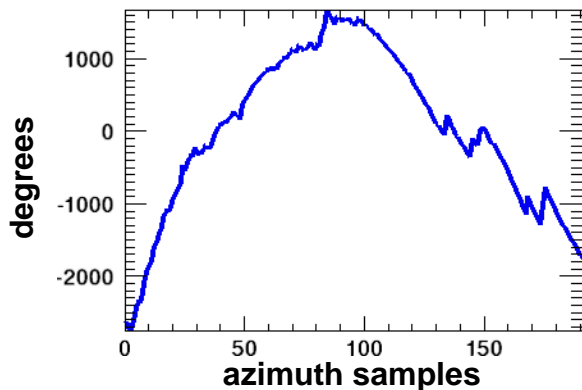
\mathbf{u}_y = slant plane azimuth unit vector

T = coherent dwell period

Δy = nominal azimuth resolution

λ = wavelength at mid band

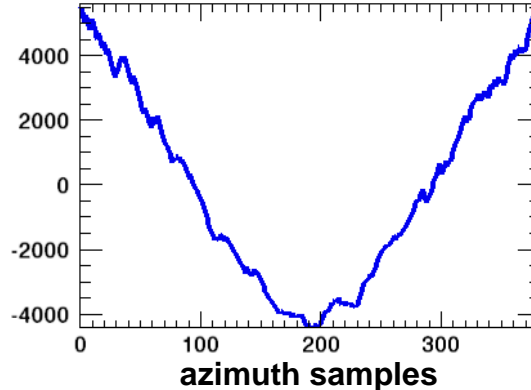
Phase Target 1



$Q = -4563$ deg GPS prediction

$Q \sim -4000$ deg observed above

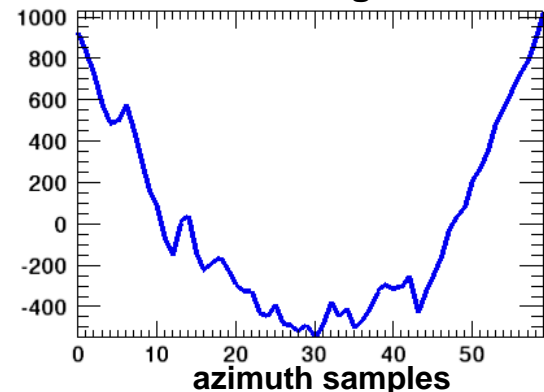
Phase Target 5



No GPS data for prediction

$Q \sim 8000$ deg observed above

Phase Target 6



$Q = 1627$ deg GPS prediction*

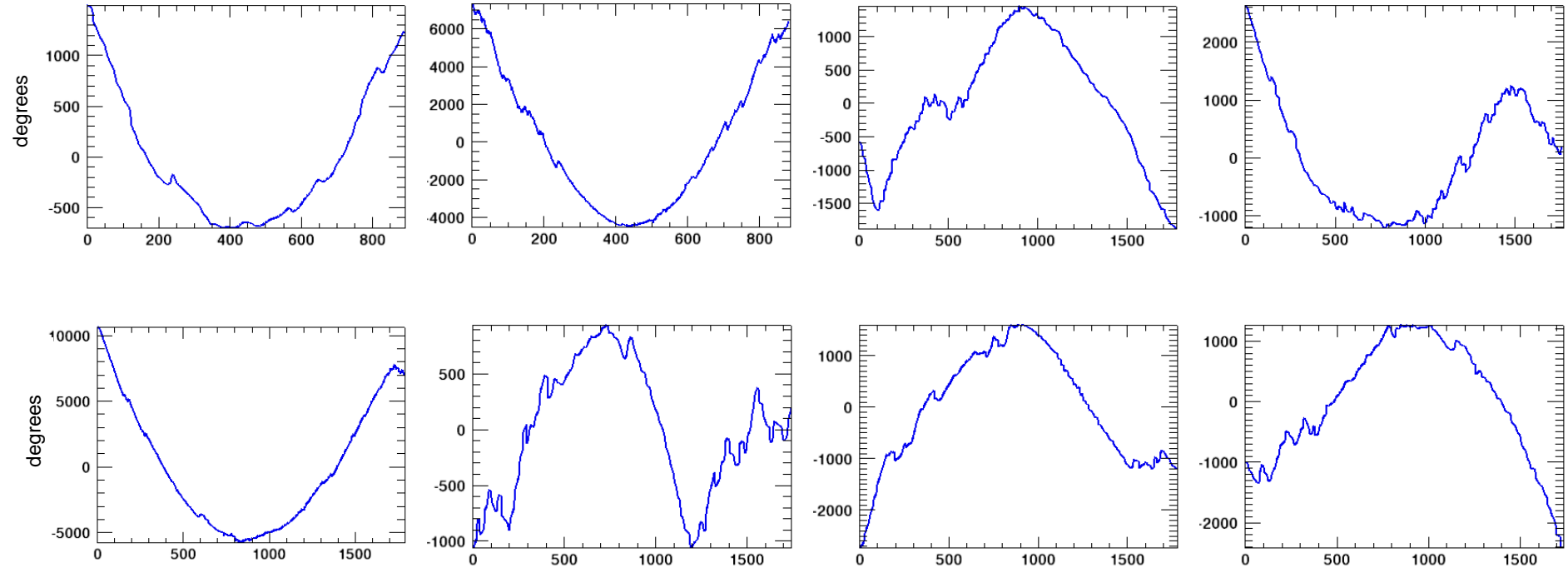
$Q \sim 1500$ deg observed above

*GPS derived acceleration set = 0

aircraft data



Moving Target Phase: Aircraft Data Observations



Quadratic Phase: target range acceleration & cross range velocity, ...

Cubic Phase: target cross range acceleration & non-constant range acceleration

Stationary targets do not have these phase signatures

GMTI

- Show examples of common processing of multiple channel radar data into image and moving target products
 - Long coherent dwell (e.g., 2 to 3 seconds)
 - Subdivision of dwell into short coherent processing intervals (e.g., 10 CPIs each 0.2 seconds duration)
- Data observations and discussions
 - MTI with and without clutter suppression
 - Target range acceleration and cross range velocity provides phase characteristics not shared stationary targets
 - Energy migration through freq bins, intrinsically more degrees of freedom to match signal, signal processing implications
 - Also hedge against false alarms

Space-Time Adaptive Processing (STAP) Formulated for SAR Imagery

Assume a system with N displaced along track antenna elements or N azimuth beams (N channels)

$$\boldsymbol{\sigma} = \boldsymbol{\sigma}(x, y) = [\sigma_1(x, y), \sigma_2(x, y), \dots, \sigma_N(x, y)]^T \quad (\text{stack or vector of images, one from each channel})$$

$$\mathbf{R} = \mathbf{R}_c + \mathbf{R}_n \quad (\text{N by N clutter plus receiver noise covariance matrix})$$

$$\mathbf{w} = [w_1, w_2, \dots, w_N] \quad (\text{channel summation weights})$$

$$\mathbf{s} = [s_1, s_2, \dots, s_N] \quad (\text{target steering vector, complex exponential of linear phase or azimuth beam weights})$$

$$s_n = \exp(i(2\pi/\lambda)(n-1)(d/r)(\mathbf{u}_d \cdot \mathbf{x})) \quad (\text{nominal antenna element space representation, angle of arrival related})$$

d = dist between antenna elements,

r = range,

\mathbf{u}_d = unit vector defines direction along which the elements are located in 3D

$$\text{SINR}(\mathbf{w}) = \frac{|\mathbf{w}^H \mathbf{s}|^2}{\mathbf{w}^H \mathbf{R} \mathbf{w}} \quad (\text{signal - to - interference ratio, include consideration to clutter power})$$

optimal $\mathbf{w} = \mathbf{R}^{-1} \mathbf{s}$ (STAP weight vector for maximum SINR, estimate \mathbf{R} from data, exclude movers)

$$\max \text{SINR}(\mathbf{w}) = \text{SINR}(\mathbf{R}^{-1} \mathbf{s}) = \left| (\mathbf{R}^{-1} \mathbf{s})^H \mathbf{s} \right| \quad (\text{max SINR, application of Cauchy - Schwarz inequality})$$

$$\text{STAP filter output} = \mathbf{w}^H \boldsymbol{\sigma} = (\mathbf{R}^{-1} \mathbf{s})^H \boldsymbol{\sigma} = \mathbf{s}^H \mathbf{R}^{-1} \boldsymbol{\sigma} \quad (\text{for a given target steering vector hypothesis})$$

application of inverse covariance matrix to image stack apparently suppresses clutter

clutter suppressed image stack = $(\mathbf{R}^{-1} \boldsymbol{\sigma})(x, y)$, (for analysis, now apply hypothesis space of steering vectors)



Element Space: 1 and 2 of 8 Clutter Images

1 and 2 of 8 channels/images shown
single look complex

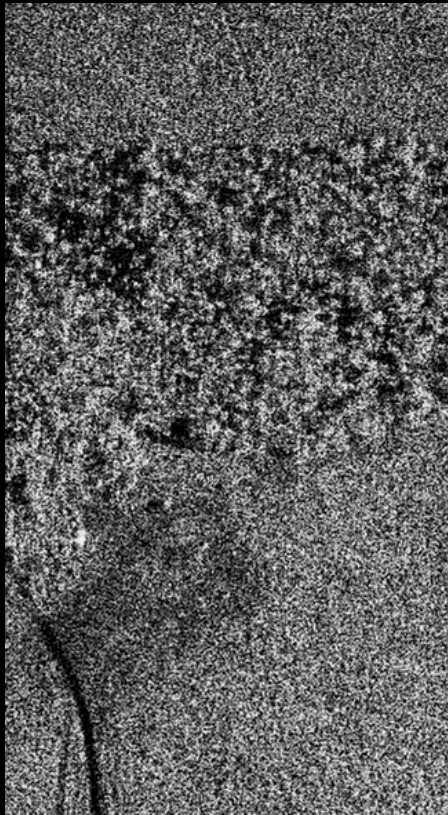


image 1

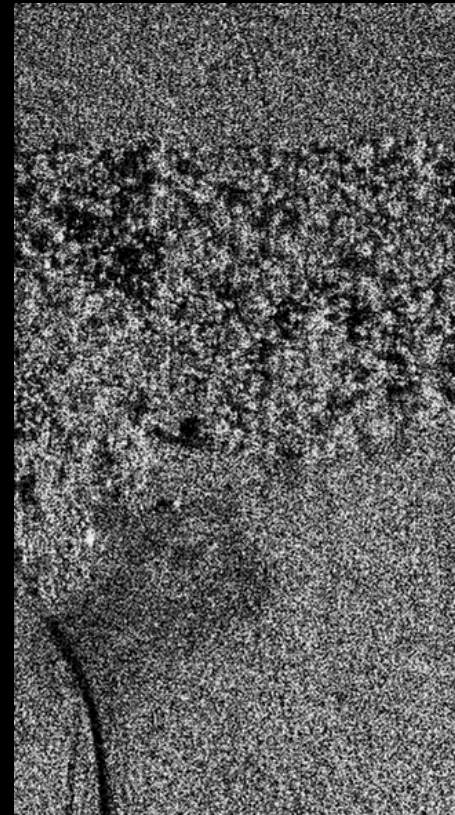


image 2

R⁻¹ Applied - Clutter Suppression Apparent

1 and 2 of 8 channels/images shown
steering vector not applied



image 1



image 2

R⁻¹ Applied - Clutter Suppression Apparent

1 and 2 of 8 channels/images shown
steering vector not (yet) applied

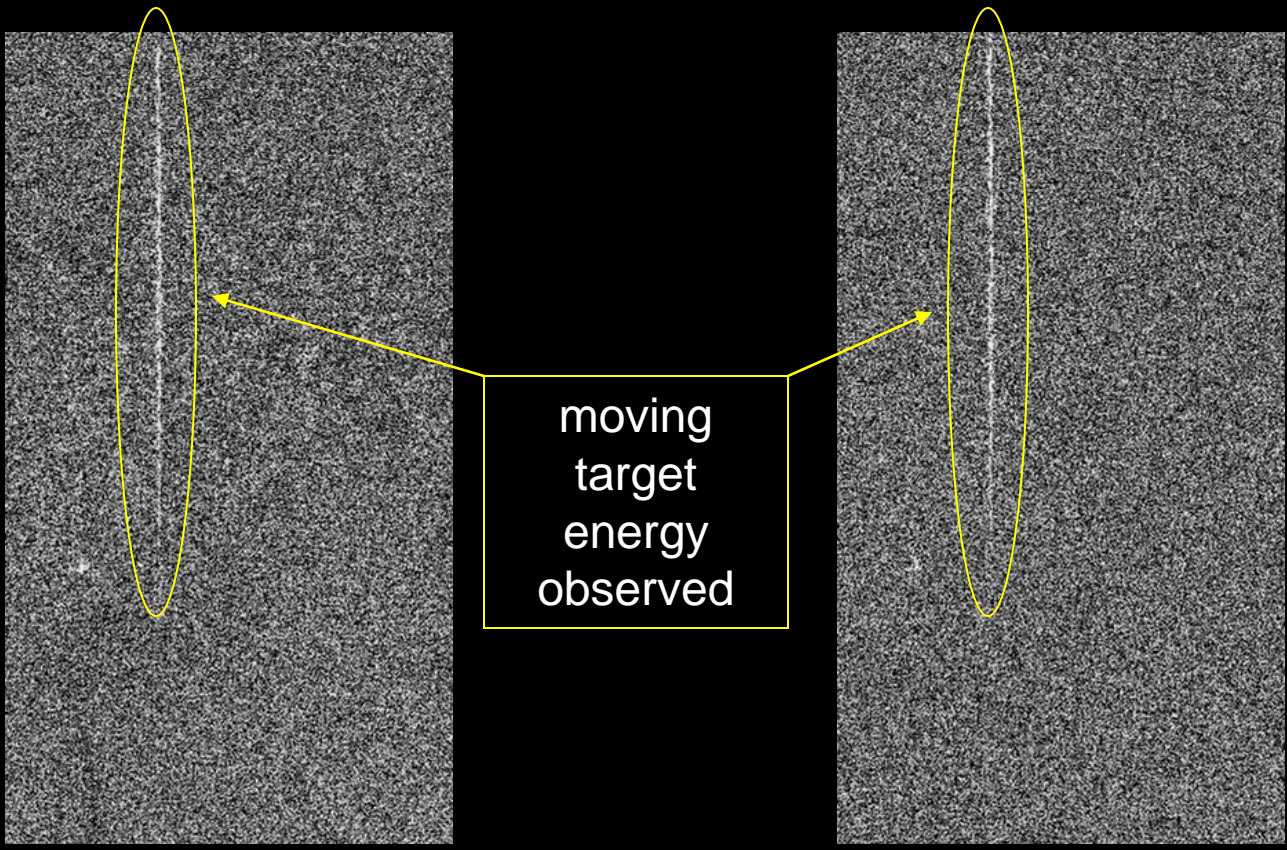


image 1

image 2



Digital Beam Steer to Upper Part of Image

Application of beam steering vector shown

Complex-valued beam steering vector components are complex sinusoids a phase which is linear with antenna element index

Analogous to discrete Fourier transform

$$\mathbf{s} = [s_1, s_2, \dots, s_N]$$

$$s_n = \exp(i (2 \pi / \lambda) (n-1) (d / r) (\mathbf{u}_d \cdot \mathbf{x}))$$



Note: Missing wavelength factor in steering vector definition corrected above on February 10, 2012.

Digital Beam Steer to Center Part of Image

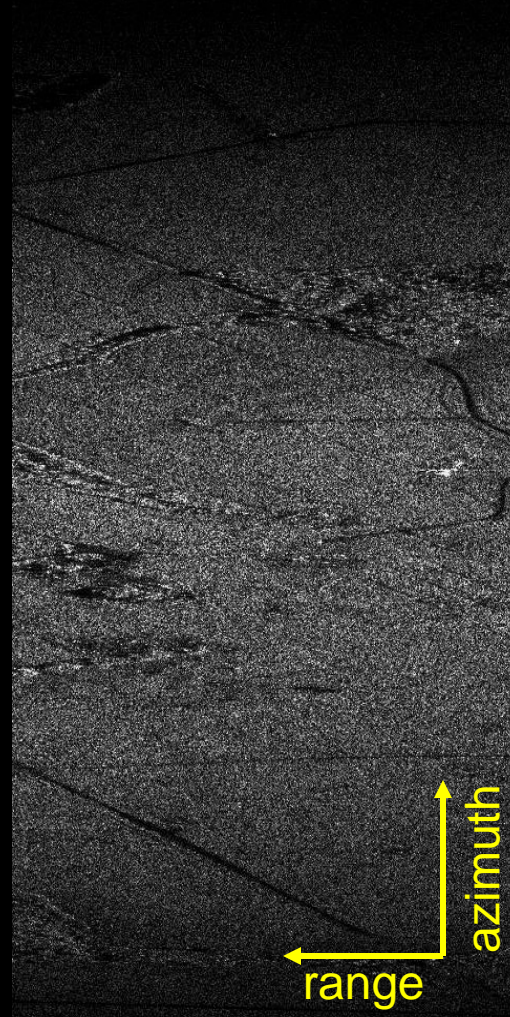
Application of beam steering vector shown

Complex-valued beam steering vector components are complex sinusoids a phase which is linear with antenna element index

Analogous to discrete Fourier transform

$$\mathbf{s} = [s_1, s_2, \dots, s_N]$$

$$s_n = \exp(i (2 \pi / \lambda) (n-1) (d / r) (\mathbf{u}_d \cdot \mathbf{x}))$$



Note: Missing wavelength factor in steering vector definition corrected above on February 10, 2012.



Digital Beam Steer to Lower Part of Image

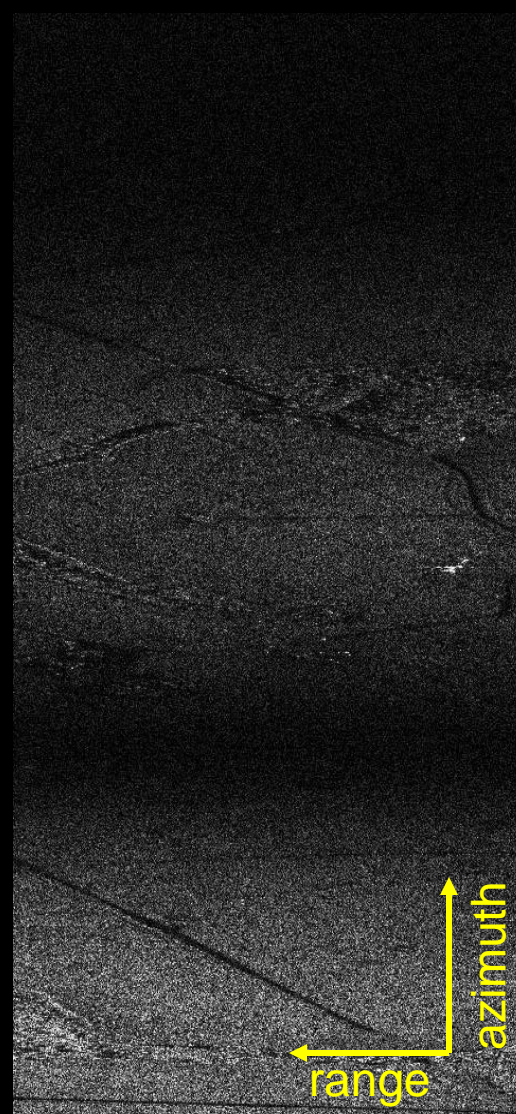
Application of beam steering vector shown

Complex-valued beam steering vector components are complex sinusoids a phase which is linear with antenna element index

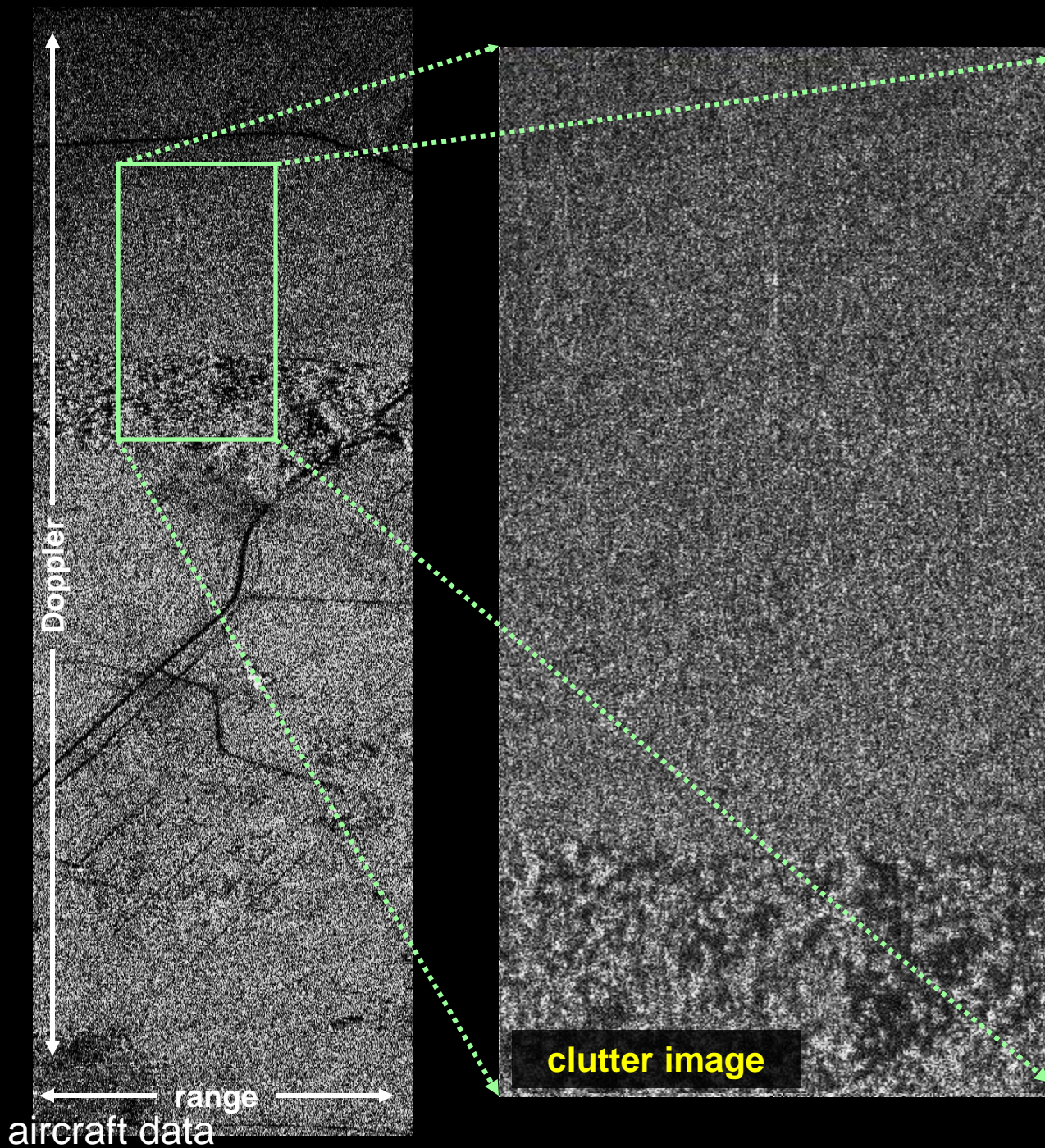
Analogous to discrete Fourier transform

$$\mathbf{s} = [s_1, s_2, \dots, s_N]$$

$$s_n = \exp(i (2 \pi / \lambda) (n-1) (d / r) (\mathbf{u}_d \cdot \mathbf{x}))$$



Note: Missing wavelength factor in steering vector definition corrected above on February 10, 2012.

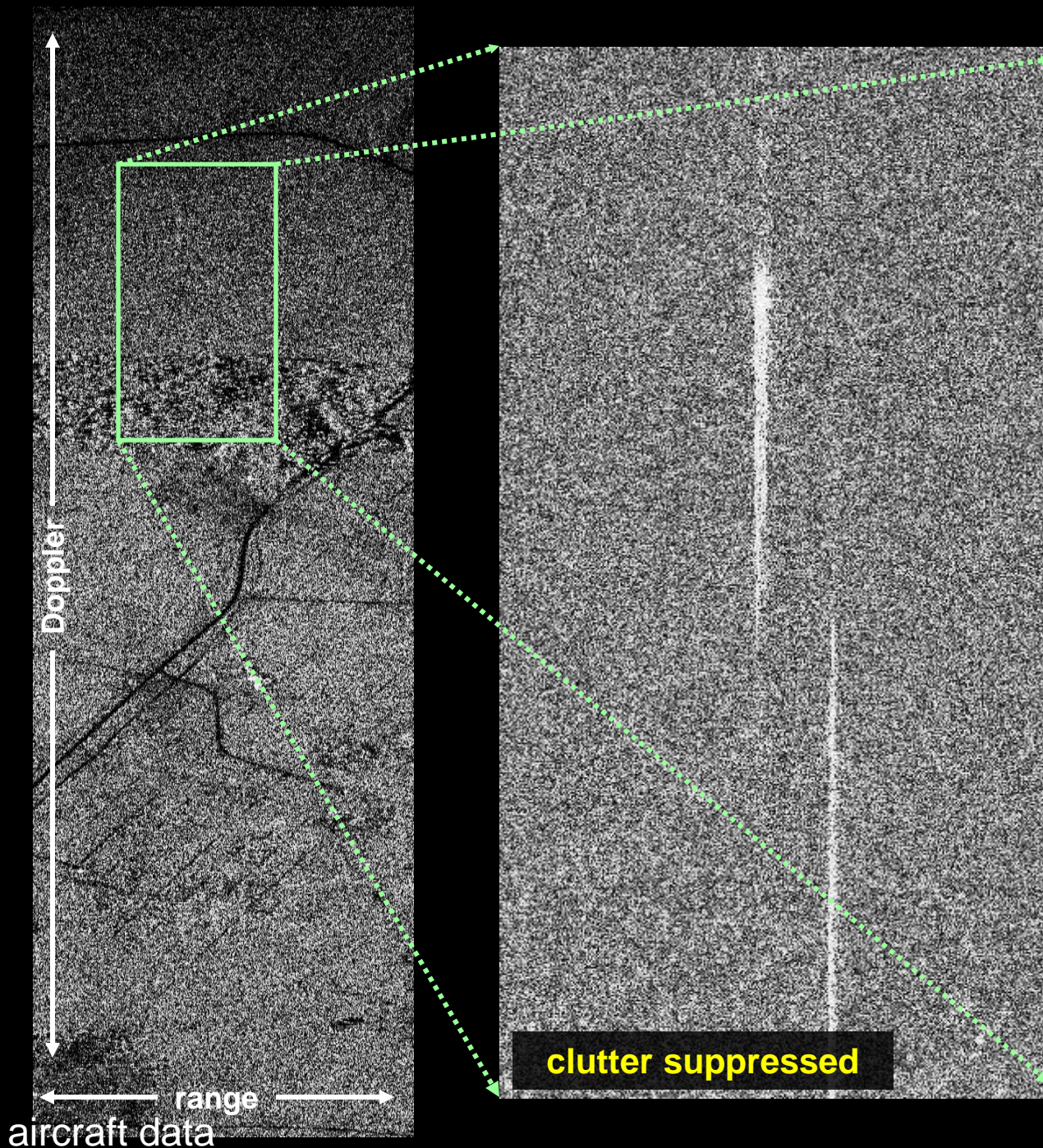


Left image shows area of interest outlined in green.

Right image is a zoom into region of interest.

Image formed with 2.7 seconds of radar dwell time.



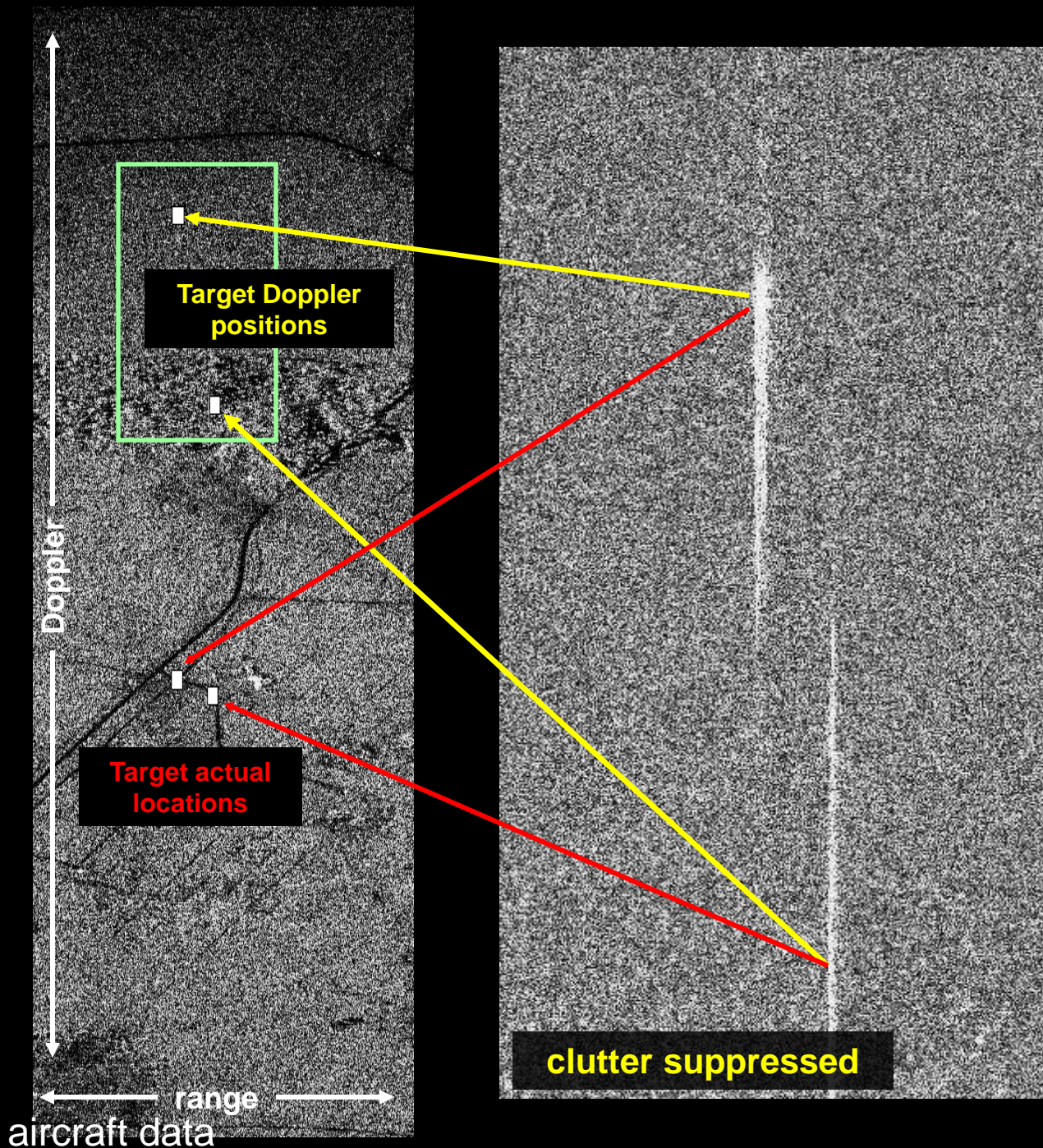


Left image shows area of interest outlined in green.

Right image results from clutter suppression processing (STAP) reveals two movers. Note energy is spread over many Doppler cells.

Multiple channels necessary for clutter suppression.





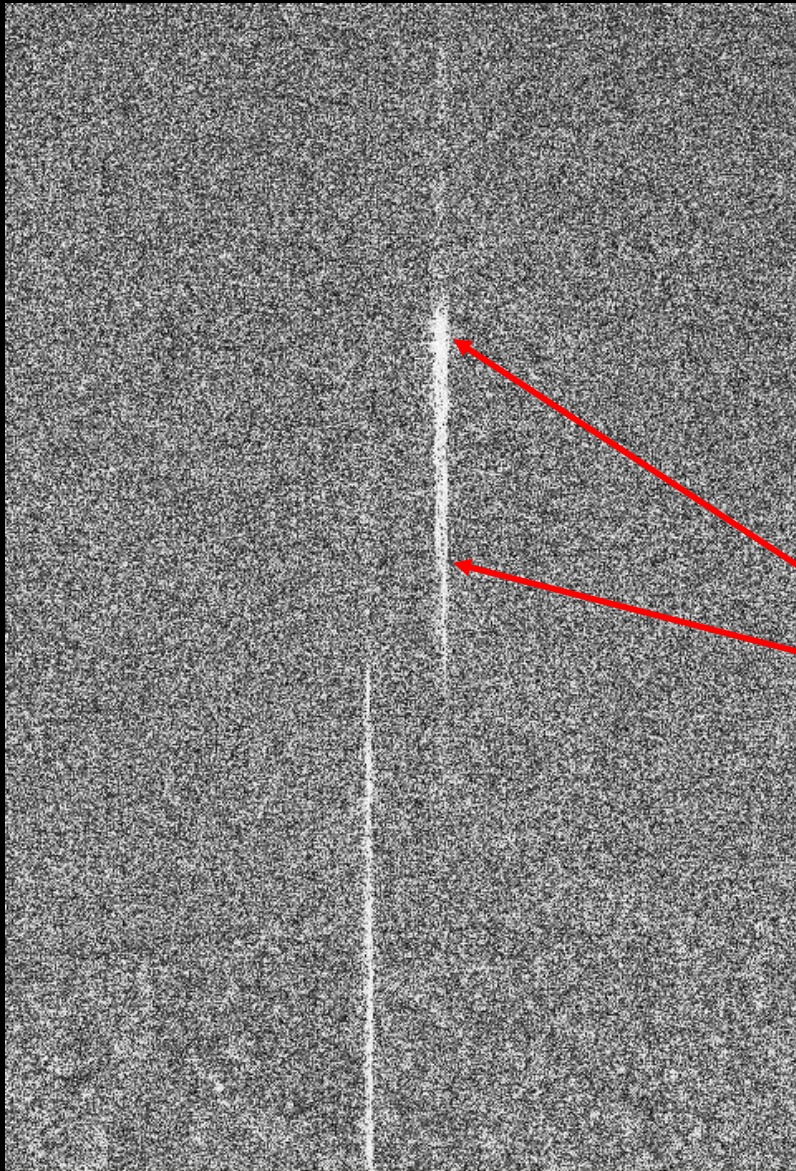
Left image shows area of interest outlined in green.

Yellow arrows point to Doppler shifted location of targets.

Red arrows point to **actual target location** as determined by radar processing algorithm (STAP).



Phase Characteristics



Clutter Suppressed Output

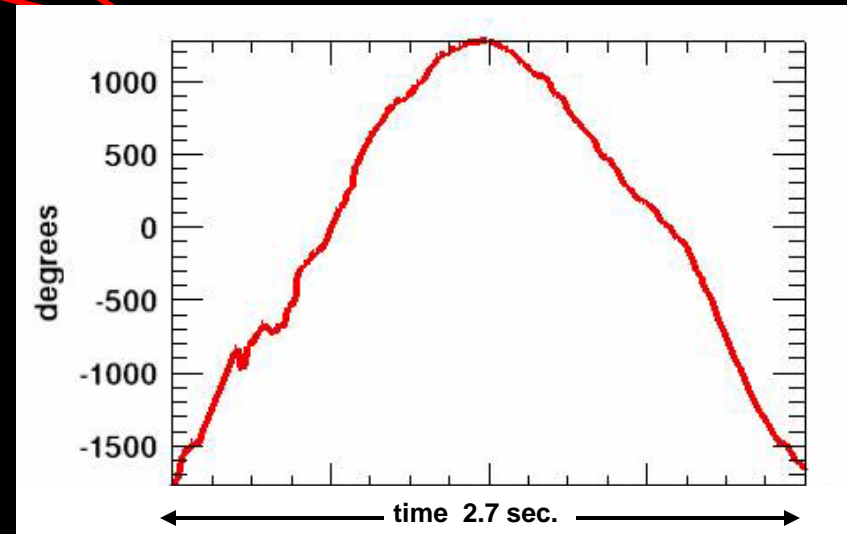
**Nominal Element Space
Adaptive Processing (STAP)**

8 channels

No quadratic phase compensation

**Quadratic Phase Frequently
Observed in Aircraft Data**

clutter suppressed - channels combined
aircraft data



Space-Time Adaptive Processing (STAP) Target Signal Loss

$$\text{SINR}(\mathbf{w}) = \frac{|\mathbf{w}^H \mathbf{s}|^2}{\mathbf{w}^H \mathbf{R} \mathbf{w}} \quad (\text{signal - to - interference ratio, include consideration to clutter power})$$

$$\text{optimal } \mathbf{w} = \mathbf{R}^{-1} \mathbf{s} \quad (\text{STAP weight vector for maximum SINR, estimate } \mathbf{R} \text{ from data, exclude movers})$$

$$\max \text{SINR}(\mathbf{w}) = \text{SINR}(\mathbf{R}^{-1} \mathbf{s}) = |(\mathbf{R}^{-1} \mathbf{s})^H \mathbf{s}| \quad (\text{max SINR, application of Cauchy - Schwarz inequality})$$

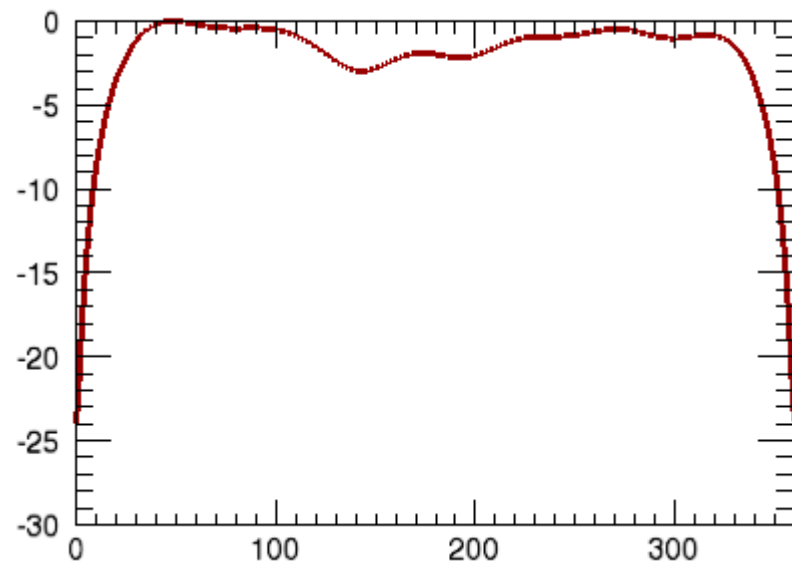
$$\text{STAP filter output} = \mathbf{w}^H \boldsymbol{\sigma} = (\mathbf{R}^{-1} \mathbf{s})^H \boldsymbol{\sigma} = \mathbf{s}^H \mathbf{R}^{-1} \boldsymbol{\sigma} \quad (\text{for a given target steering vector hypothesis})$$

$$\max \text{SNR} = |(\mathbf{R}_n^{-1} \mathbf{s})^H \mathbf{s}| \quad (\text{gives no consideration to clutter power})$$

$$\text{SINR}(\mathbf{R}^{-1} \mathbf{s}) = L_{\text{sinr}} \text{SNR} \quad (\text{SINR loss defined relative to SNR})$$

STAP SINR Loss

8 antenna element aircraft data
CNR per channel approx 18 dB



steering vector phase change per channel (deg)



Space-Time Adaptive Processing (STAP) Clutter Loss (Suppression)

$$\text{SINR}(\mathbf{w}) = \frac{|\mathbf{w}^H \mathbf{s}|^2}{\mathbf{w}^H \mathbf{R} \mathbf{w}}$$

(signal - to - interference ratio, include consideration to clutter power)

$$\text{optimal } \mathbf{w} = \mathbf{R}^{-1} \mathbf{s}$$

(STAP weight vector for maximum SINR, estimate \mathbf{R} from data, exclude movers)

$$\text{SINR}(\mathbf{R}^{-1} \mathbf{s}) = L_{\text{sinr}} \text{SNR}$$

(SINR loss defined relative to SNR)

$$\text{CNR}(\mathbf{w}) = \frac{\mathbf{w}^H \mathbf{R}_c \mathbf{w}}{\mathbf{w}^H \mathbf{R}_n \mathbf{w}} = \frac{\mathbf{w}^H (\mathbf{R} - \mathbf{R}_n) \mathbf{w}}{\mathbf{w}^H \mathbf{R}_n \mathbf{w}} = \frac{\mathbf{w}^H \mathbf{R} \mathbf{w}}{\mathbf{w}^H \mathbf{R}_n \mathbf{w}} - 1$$

$$\mathbf{R} \mathbf{e}_k = \lambda_k \mathbf{e}_k \quad k = 1, 2, \dots, N$$

(eigenvectors and eigenvalues)

$$\text{CNR}(\mathbf{w}) \leq \text{CNR}(\mathbf{e}_1)$$

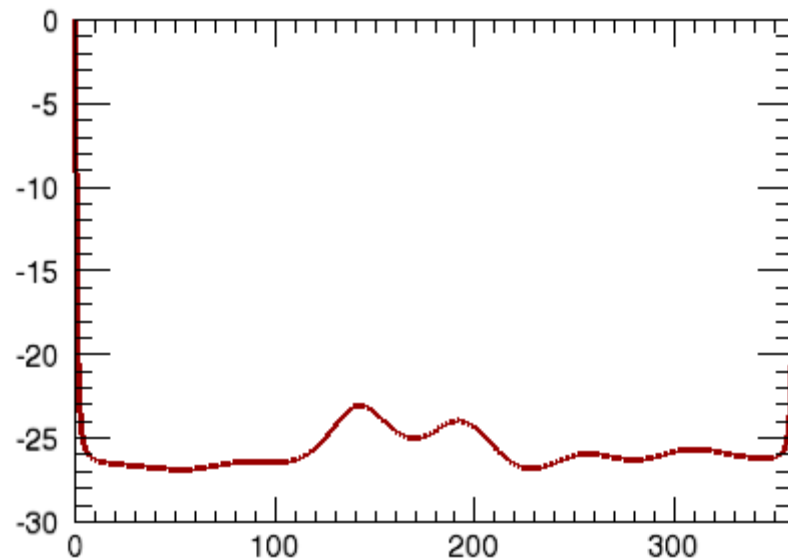
(max CNR using eigenvector with max eigenvalue as channel summation weights)

$$\text{CNR}(\mathbf{R}^{-1} \mathbf{s}) = L_c \text{CNR}(\mathbf{e}_1)$$

(defines the clutter suppression, post channel summation, relative to max CNR)

STAP Clutter Suppression

8 element aircraft data
CNR per channel approx 18 dB



steering vector phase change per channel (deg)



Analysis: Relation Between Space Time Adaptive Processing (STAP) and Eigen Image Decomposition

\mathbf{R} = N by N covariance matrix, N = number of channels

$$\mathbf{R}\mathbf{e}_k = \lambda_k \mathbf{e}_k \quad k = 1, 2, \dots, N$$

$$\mathbf{R}^{-1}\mathbf{e}_k = \lambda_k^{-1} \mathbf{e}_k$$

$$\boldsymbol{\sigma} = \boldsymbol{\sigma}(x, y) = [\sigma_1(x, y), \sigma_2(x, y), \dots, \sigma_N(x, y)]^T \quad (\text{data/image vector})$$

$$\boldsymbol{\sigma}(x, y) = \sum_k [\mathbf{e}_k^H \boldsymbol{\sigma}(x, y)] \mathbf{e}_k \quad (\text{eigenvector expansion, orthonormal basis})$$

$\mathbf{e}_k^H \boldsymbol{\sigma}(x, y)$ = eigen - image computed as kth eigenvector projected onto image vector, $k = 1, 2, \dots, N$.

$$\mathbf{w}^H \boldsymbol{\sigma} = (\mathbf{R}^{-1}\mathbf{s})^H \boldsymbol{\sigma} = \mathbf{s}^H \mathbf{R}^{-1} \boldsymbol{\sigma} = \sum_k \frac{(\mathbf{e}_k^H \boldsymbol{\sigma})}{\lambda_k} (\mathbf{s}^H \mathbf{e}_k) \quad (\text{adaptive processor \& eigenvector expansion})$$

Inverse covariance applied to image stack results in eigen image vector sum as above

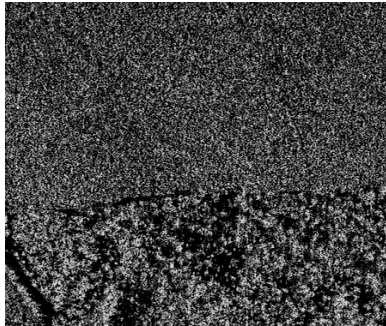
Moving target energy in eigen images, helps explain why targets are observed in suppressed imagery, following application of inverse covariance matrix to image stack

Optimal adaptive processor (STAP) is expressed as weighted sum of eigen images, as given above (applies to element & beam space)



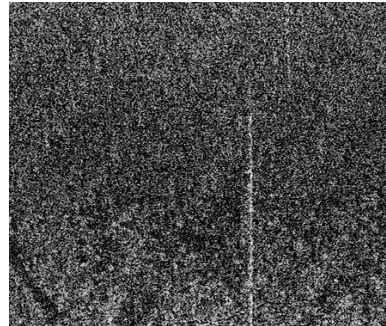
Relation Between Space Time Adaptive Processing (STAP) and Eigen Image Decomposition

$\mathbf{e}_1^H \boldsymbol{\sigma}(x, y)$



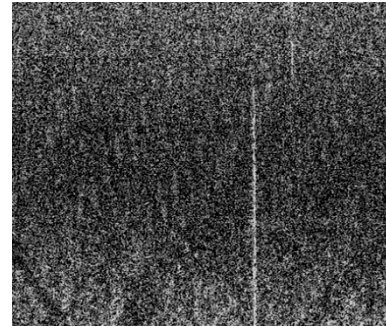
$\hat{\lambda} = 7.6169$

$\mathbf{e}_2^H \boldsymbol{\sigma}(x, y)$



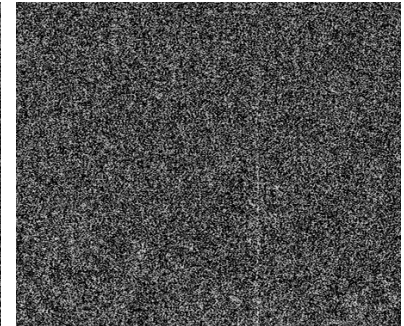
$\hat{\lambda} = 0.1220$

$\mathbf{e}_3^H \boldsymbol{\sigma}(x, y)$



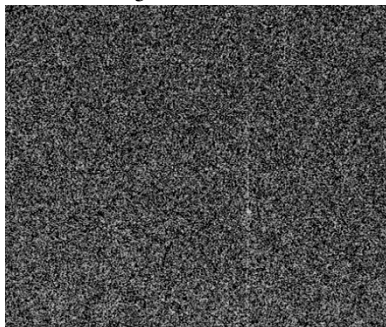
$\hat{\lambda} = 0.0818$

$\mathbf{e}_4^H \boldsymbol{\sigma}(x, y)$



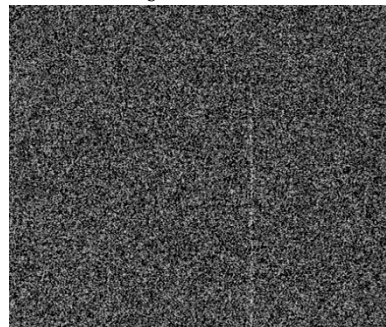
$\hat{\lambda} = 0.0518$

$\mathbf{e}_5^H \boldsymbol{\sigma}(x, y)$



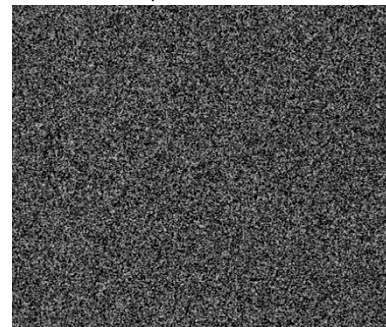
$\hat{\lambda} = 0.0427$

$\mathbf{e}_6^H \boldsymbol{\sigma}(x, y)$



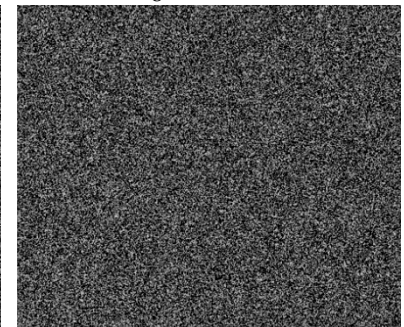
$\hat{\lambda} = 0.0306$

$\mathbf{e}_7^H \boldsymbol{\sigma}(x, y)$



$\hat{\lambda} = 0.0273$

$\mathbf{e}_8^H \boldsymbol{\sigma}(x, y)$



$\hat{\lambda} = 0.0266$

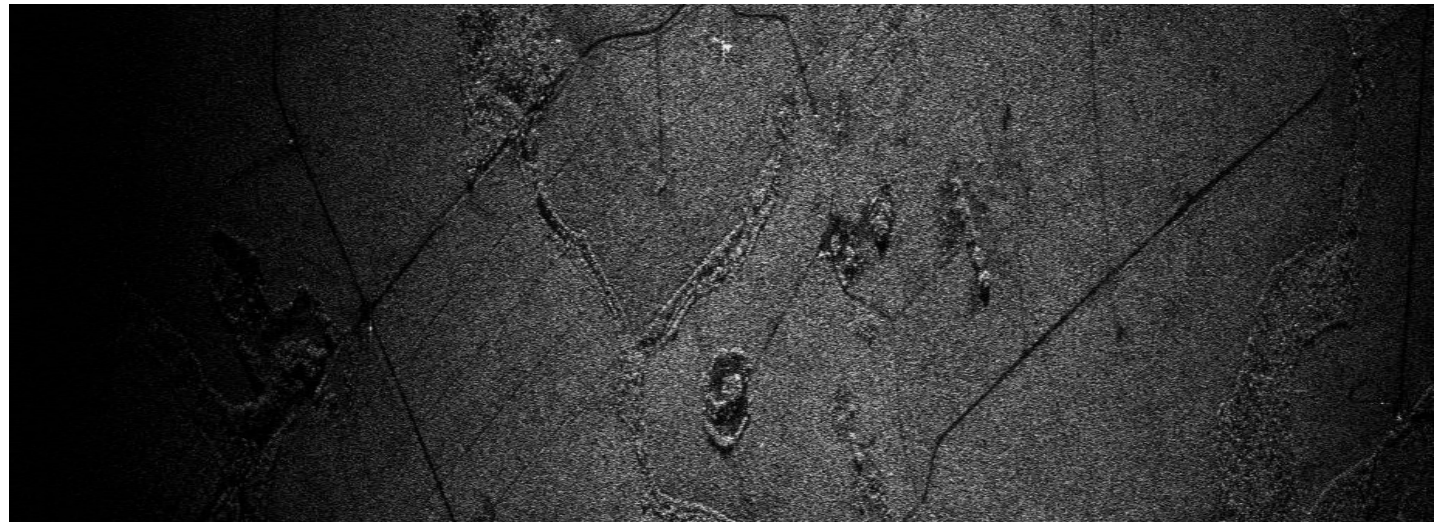
$$\mathbf{w}^H \boldsymbol{\sigma} = (\mathbf{R}^{-1} \mathbf{s})^H \boldsymbol{\sigma} = \mathbf{s}^H \mathbf{R}^{-1} \boldsymbol{\sigma} = \sum_k \frac{(\mathbf{e}_k^H \boldsymbol{\sigma})}{\lambda_k} (\mathbf{s}^H \mathbf{e}_k)$$

Analysis: Optimal Adaptive Processor is Weighted Sum of Eigen-Images

Observation: Variability of Eigenvalues with CNR

Beam Edge

Bright Uniform Clutter



Eigenvalues of R

ratio
largest/smallest
eigenvalues = 26

5.9598164
0.46193165
0.31020248
0.28341122
0.26182939
0.25569636
0.24116470
0.22594751

Eigenvalues of R

ratio
largest/smallest
eigenvalues = 286

7.6169138
0.12200656
0.081824081
0.051896852
0.042732919
0.030645195
0.027344463
0.026636630

Greater range of variability of eigenvalues observed for bright clutter

Summary Space-Time Adaptive Processing (STAP) Formulated for SAR Imagery

Assume a system with N displaced along track antenna elements or N azimuth beams (N channels)

$$\text{SINR}(\mathbf{w}) = \frac{|\mathbf{w}^H \mathbf{s}|^2}{\mathbf{w}^H \mathbf{R} \mathbf{w}} \quad (\text{signal - to - interference ratio, include consideration to clutter power})$$

optimal $\mathbf{w} = \mathbf{R}^{-1} \mathbf{s}$ (STAP weight vector for maximum SINR, estimate \mathbf{R} from data, exclude movers)

$$\max \text{SINR}(\mathbf{w}) = \text{SINR}(\mathbf{R}^{-1} \mathbf{s}) = \left| (\mathbf{R}^{-1} \mathbf{s})^H \mathbf{s} \right| \quad (\text{max SINR, application of Cauchy - Schwarz inequality})$$

STAP filter output = $\mathbf{w}^H \boldsymbol{\sigma} = (\mathbf{R}^{-1} \mathbf{s})^H \boldsymbol{\sigma} = \mathbf{s}^H \mathbf{R}^{-1} \boldsymbol{\sigma}$ (for a given target steering vector hypothesis)

application of inverse covariance matrix to image stack apparently suppresses clutter

clutter suppressed image stack = $(\mathbf{R}^{-1} \boldsymbol{\sigma})(x, y)$

$$\max \text{SNR} = \left| (\mathbf{R}_n^{-1} \mathbf{s})^H \mathbf{s} \right| \quad (\text{gives no consideration to clutter power})$$

$\text{SINR}(\mathbf{R}^{-1} \mathbf{s}) = L_{\text{sinr}} \text{SNR}$ (SINR loss defined relative to SNR)

$$\text{CNR}(\mathbf{w}) = \frac{\mathbf{w}^H \mathbf{R}_c \mathbf{w}}{\mathbf{w}^H \mathbf{R}_n \mathbf{w}} = \frac{\mathbf{w}^H (\mathbf{R} - \mathbf{R}_n) \mathbf{w}}{\mathbf{w}^H \mathbf{R}_n \mathbf{w}} = \frac{\mathbf{w}^H \mathbf{R} \mathbf{w}}{\mathbf{w}^H \mathbf{R}_n \mathbf{w}} - 1$$

$\mathbf{R} \mathbf{e}_k = \lambda_k \mathbf{e}_k \quad k = 1, 2, \dots, N$ (eigenvectors and eigenvalues)

$\text{CNR}(\mathbf{w}) \leq \text{CNR}(\mathbf{e}_1)$ (max CNR using eigenvector with max eigenvalue as channel summation weights)

$\text{CNR}(\mathbf{R}^{-1} \mathbf{s}) = L_c \text{CNR}(\mathbf{e}_1)$ (defines the clutter suppression, post channel summation, relative to max CNR)

$$\mathbf{R}^{-1} \mathbf{e}_k = \lambda_k^{-1} \mathbf{e}_k$$

$$\boldsymbol{\sigma}(x, y) = \sum_k [\mathbf{e}_k^H \boldsymbol{\sigma}(x, y)] \mathbf{e}_k \quad (\text{eigenvector expansion, orthonormal basis})$$

$\mathbf{e}_k^H \boldsymbol{\sigma}(x, y) =$ eigen - image computed as kth eigenvector projected onto image vector, $k = 1, 2, \dots, N$.

$$\mathbf{w}^H \boldsymbol{\sigma} = (\mathbf{R}^{-1} \mathbf{s})^H \boldsymbol{\sigma} = \mathbf{s}^H \mathbf{R}^{-1} \boldsymbol{\sigma} = \sum_k \frac{(\mathbf{e}_k^H \boldsymbol{\sigma})}{\lambda_k} (\mathbf{s}^H \mathbf{e}_k) \quad (\text{adaptive processor \& eigenvector expansion})$$



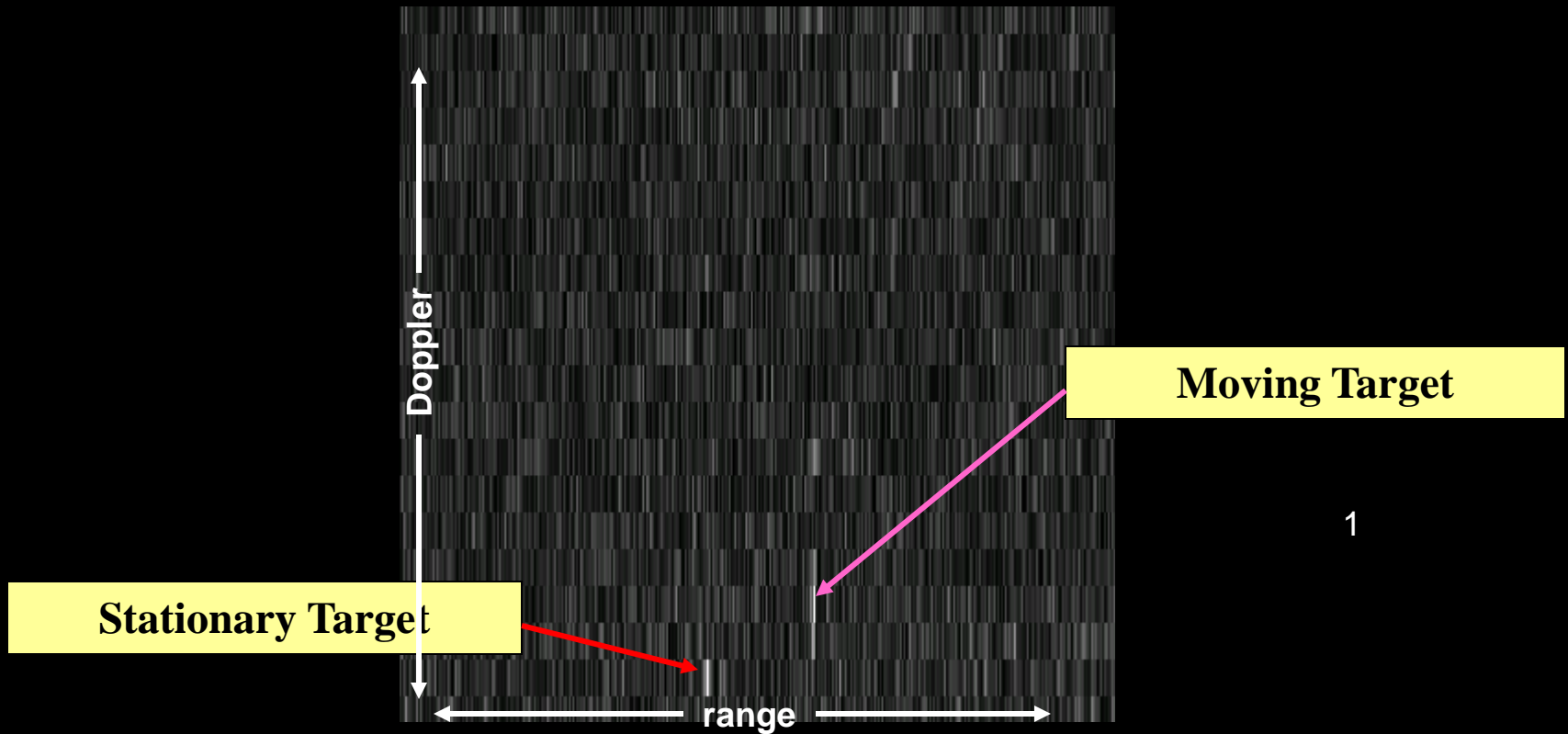
Last Example: Show Moving Target Quadratic Phase Causes Target Energy to Migrate Through Doppler/Azimuth Cells

Single Coherent Data Collection Period (2.7 sec.) Divided into 13 Time Intervals

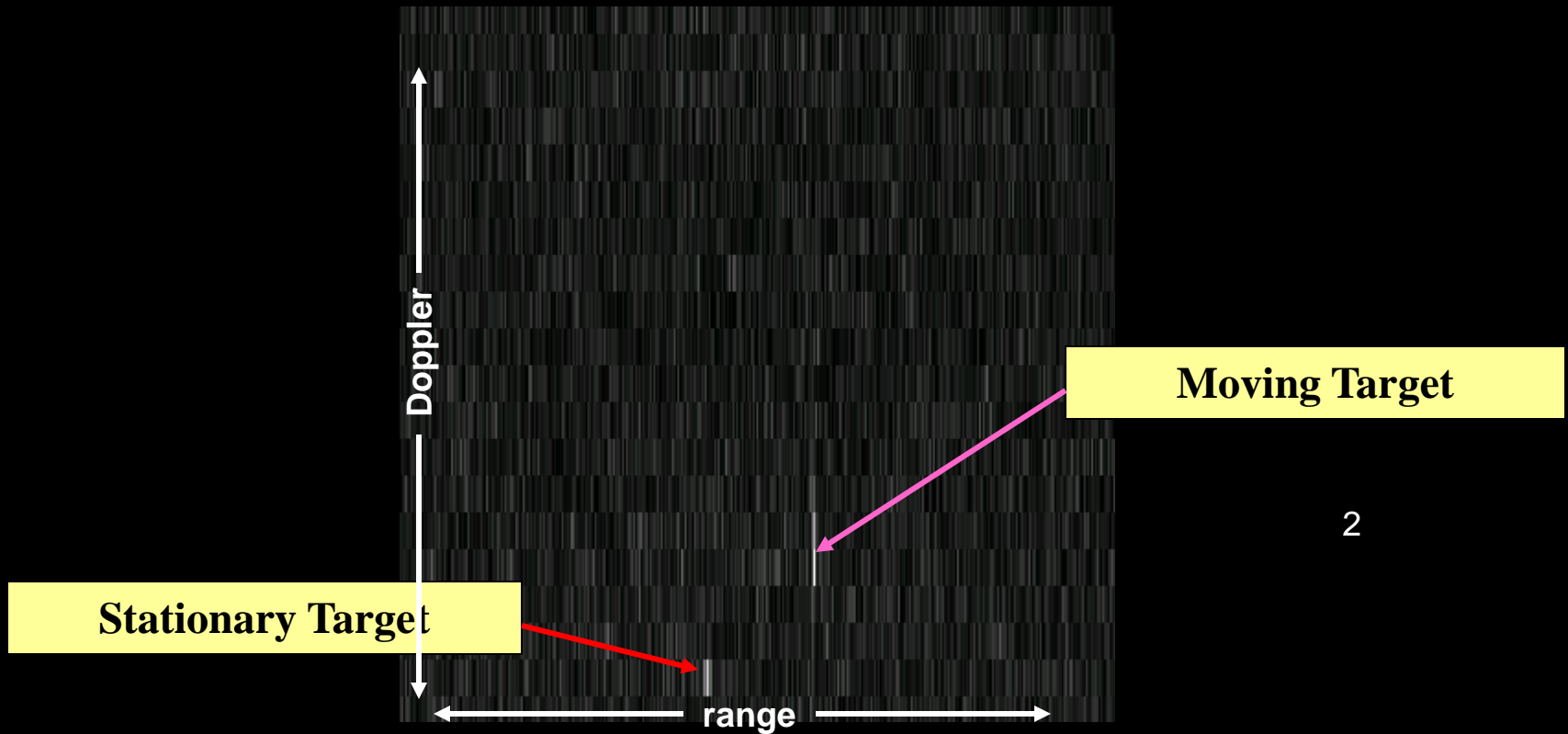
For each time interval 8 channels are processed via STAP and Displayed as a Time Sequenced Movie of 13 Images (azimuth resolution more coarse by factor of 13)

Note that SAR image formation applied to the full data collection period, then subdividing the data, mitigates moving target migration through range bins

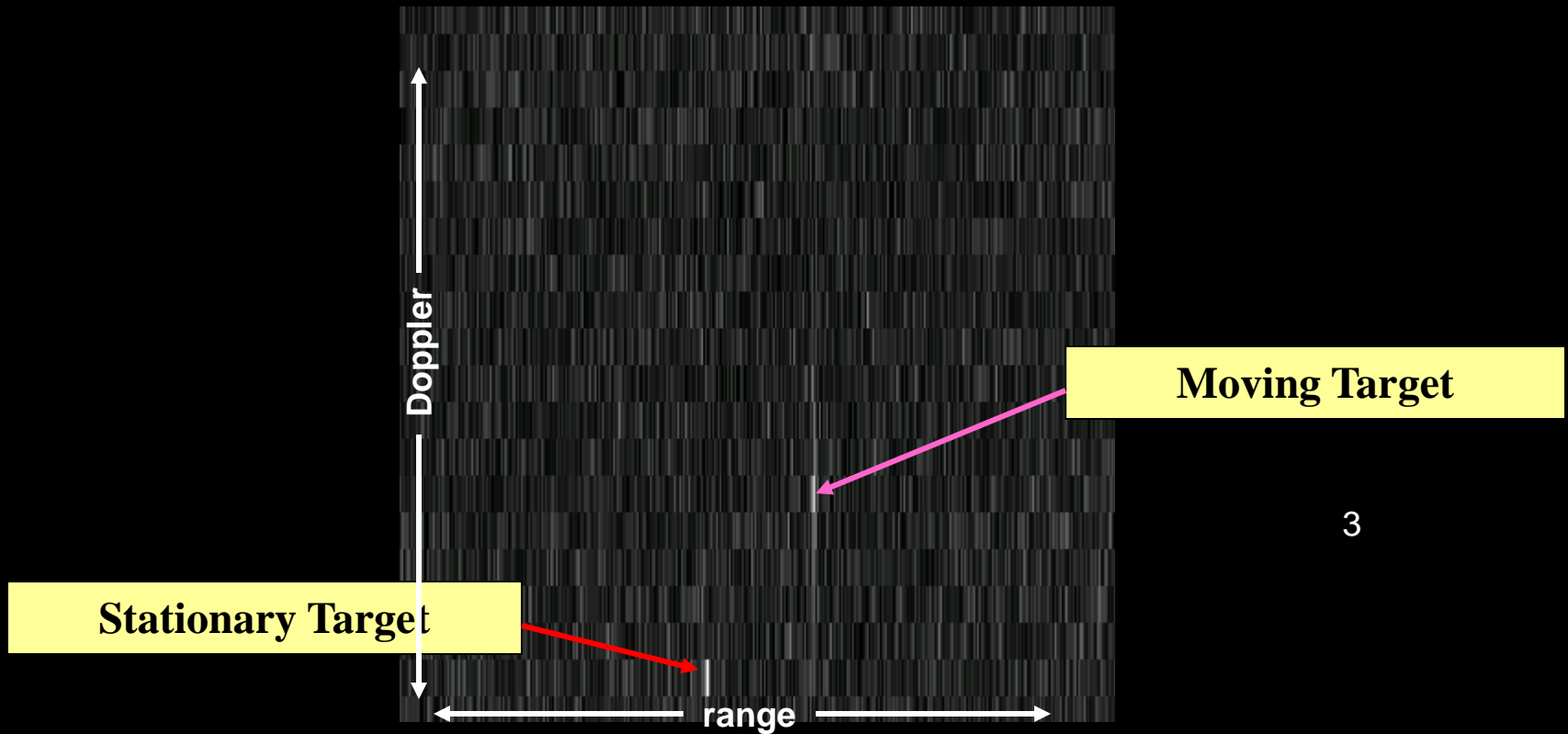
Moving Target Observed in Clutter Suppressed Imagery



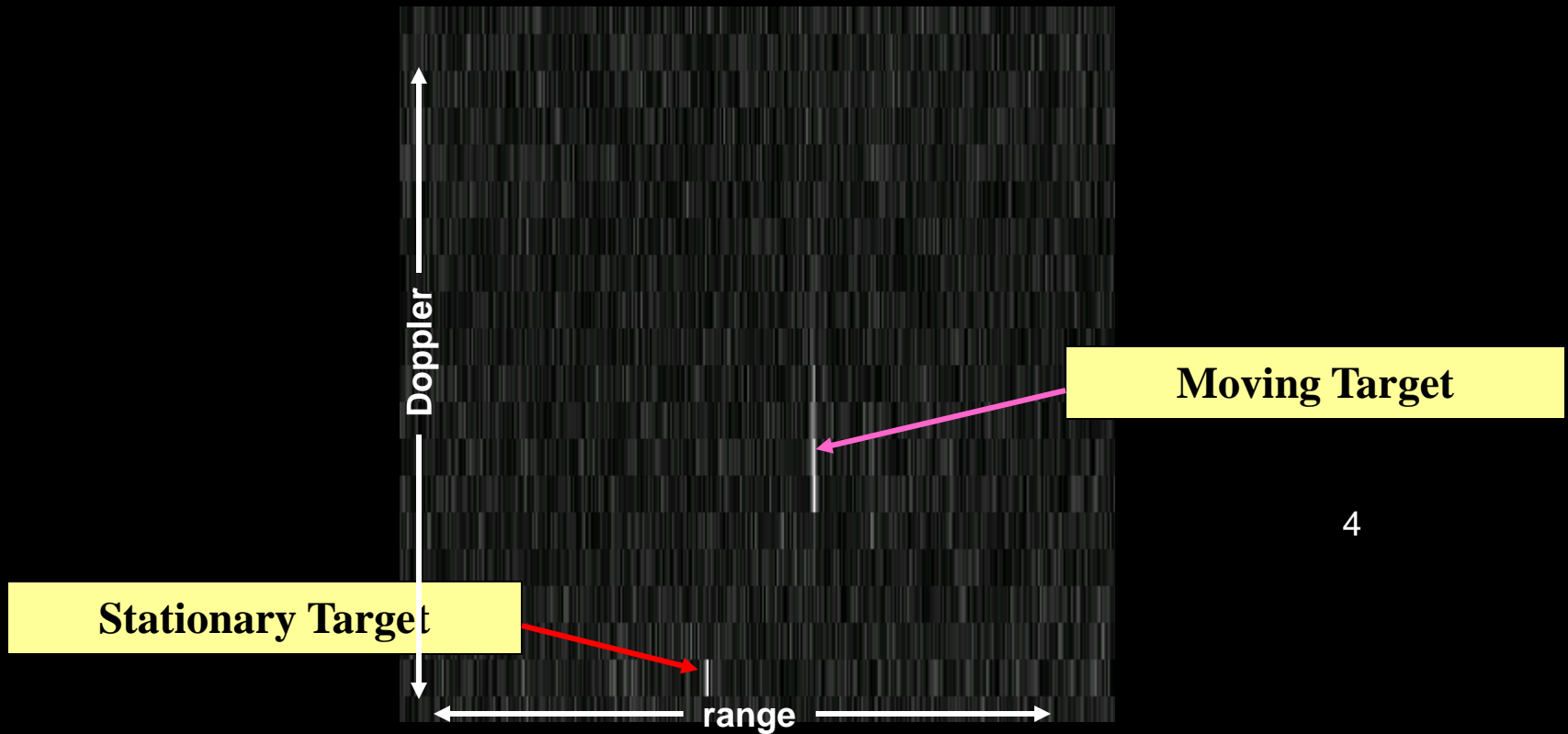
Moving Target Observed in Clutter Suppressed Imagery



Moving Target Observed in Clutter Suppressed Imagery



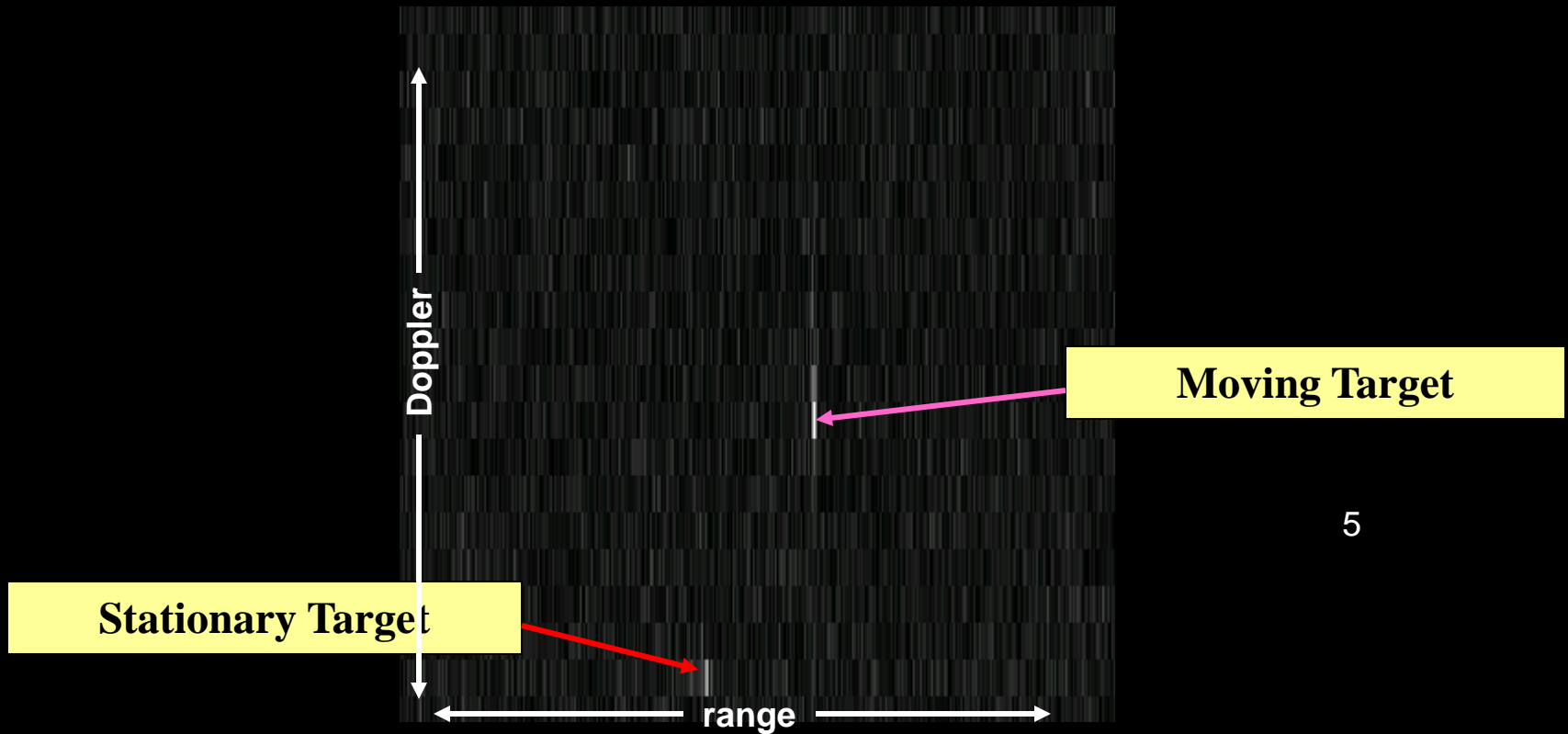
Moving Target Observed in Clutter Suppressed Imagery



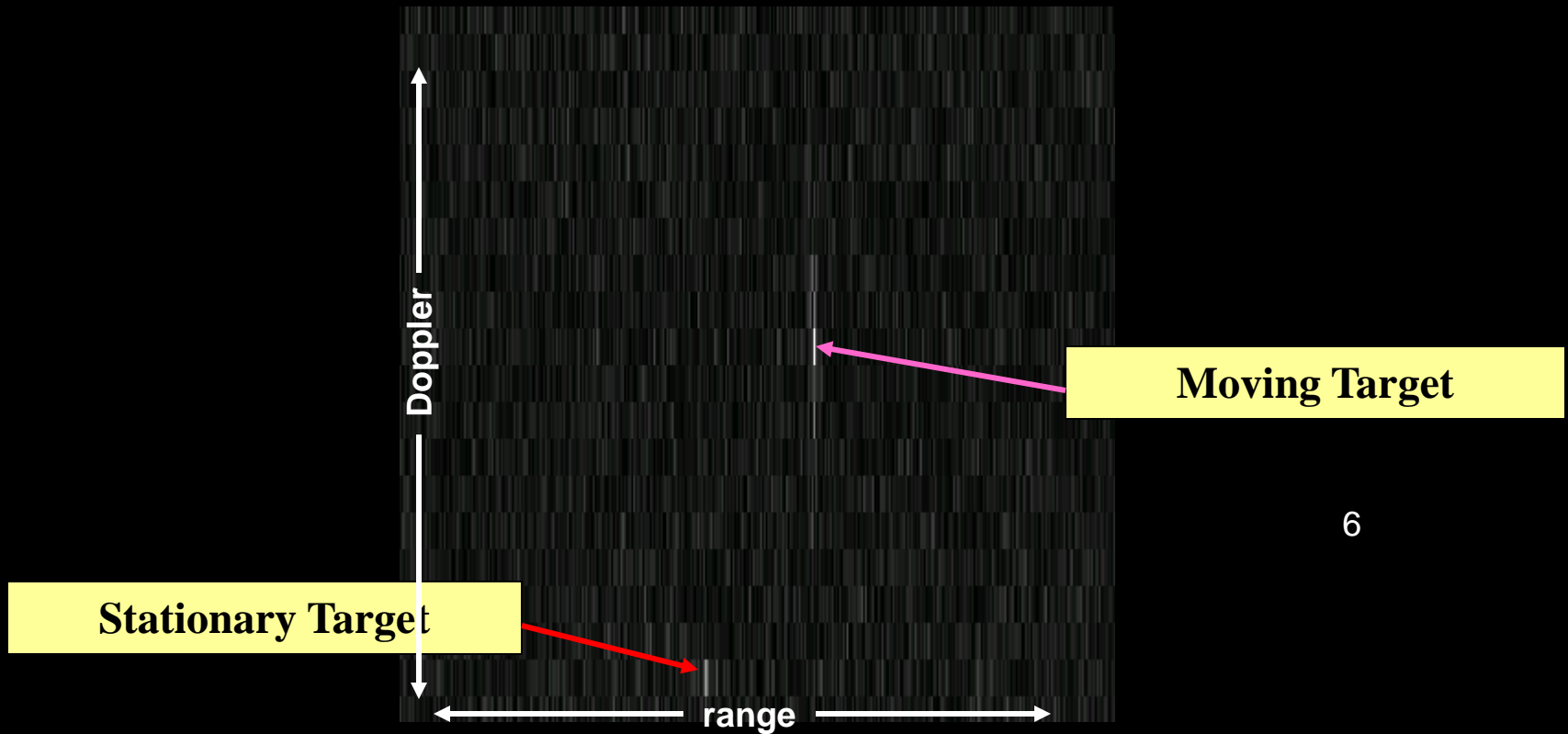
4



Moving Target Observed in Clutter Suppressed Imagery



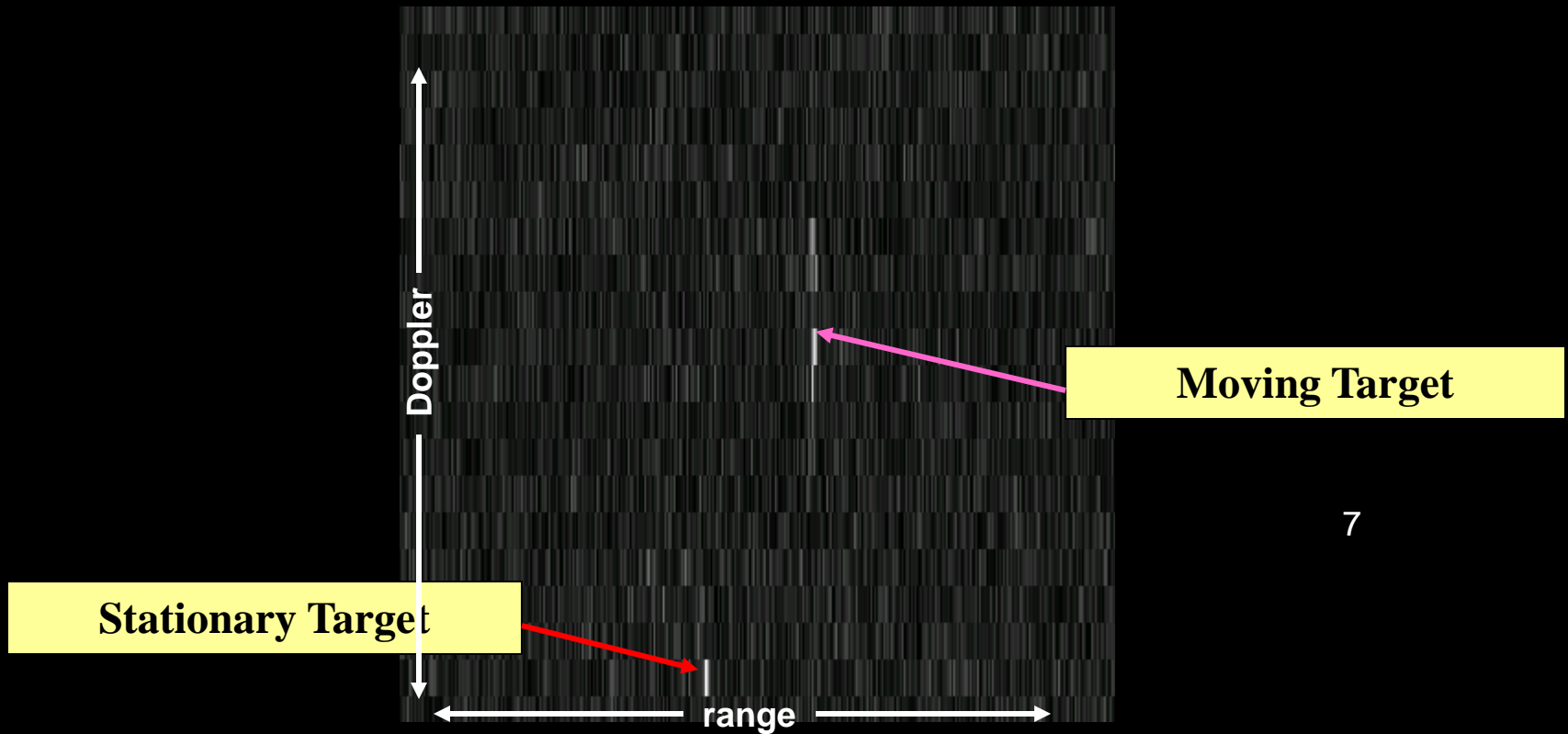
Moving Target Observed in Clutter Suppressed Imagery



6



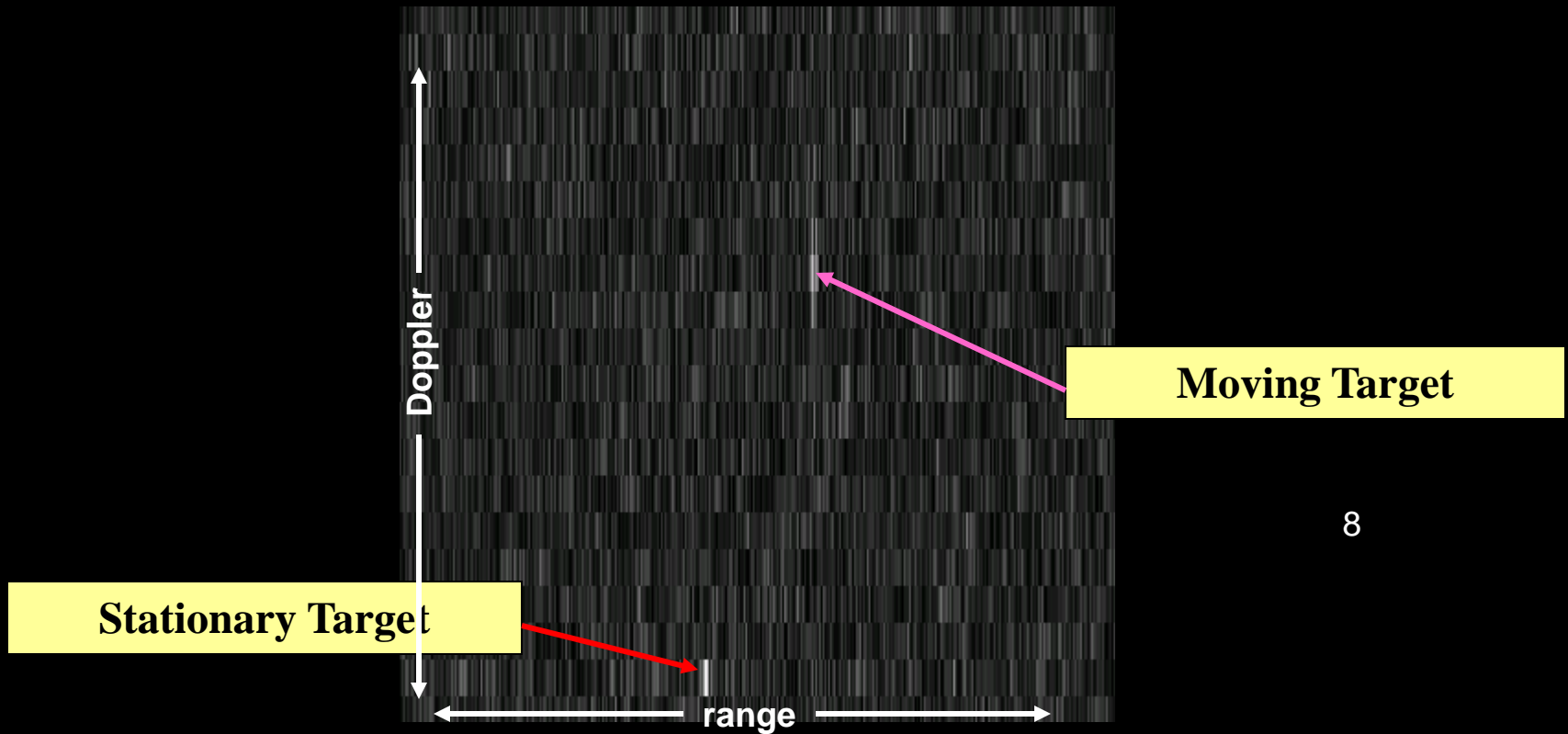
Moving Target Observed in Clutter Suppressed Imagery



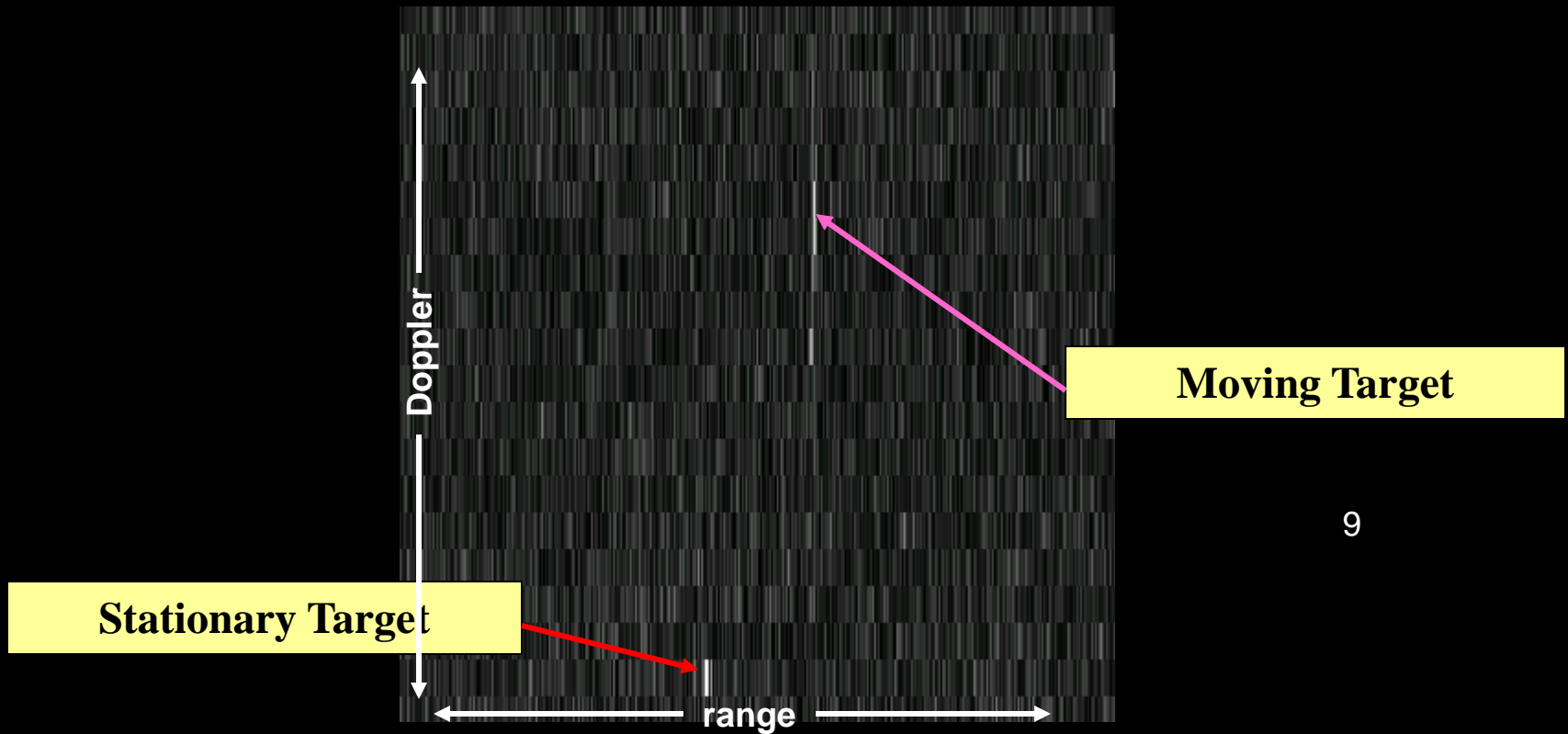
7



Moving Target Observed in Clutter Suppressed Imagery



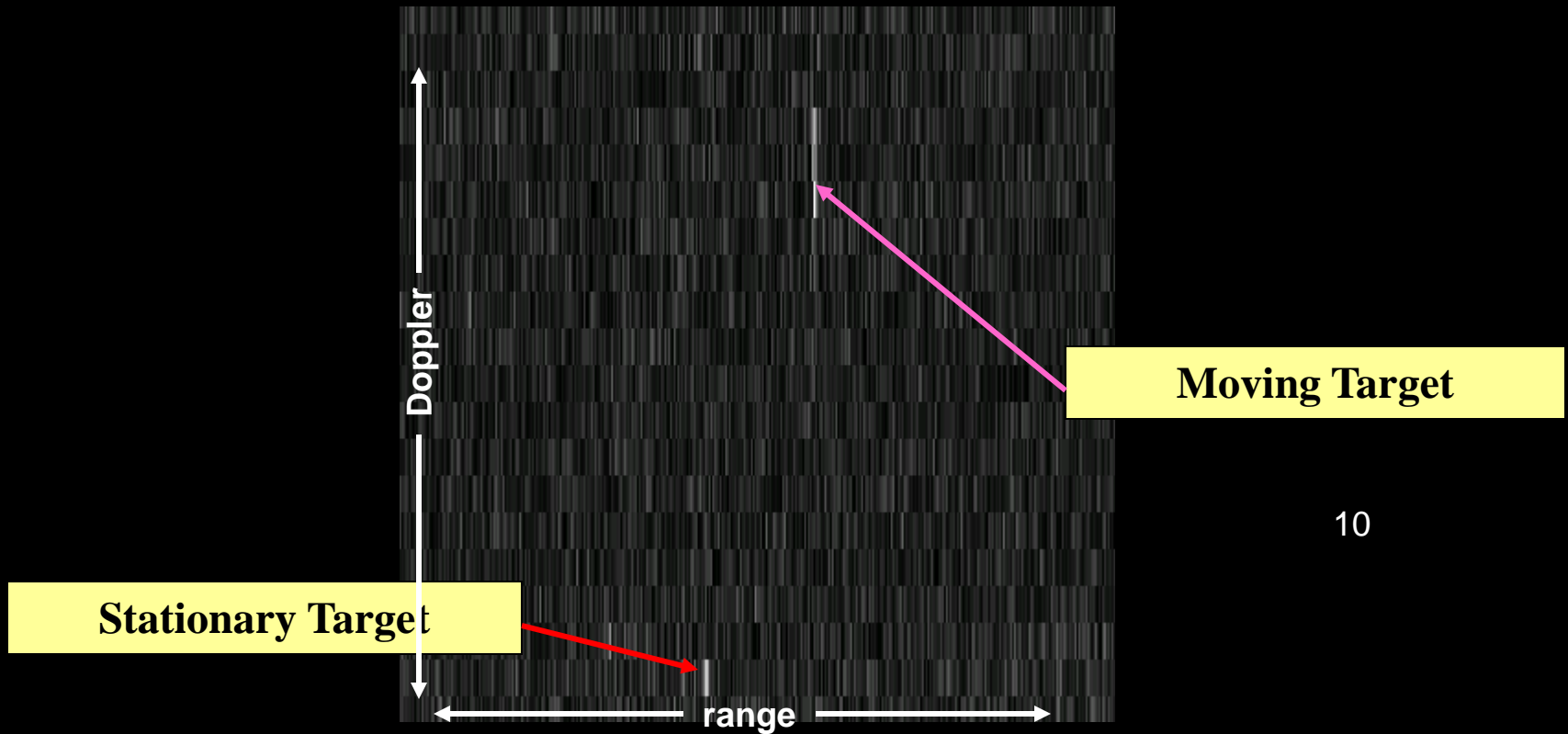
Moving Target Observed in Clutter Suppressed Imagery



9



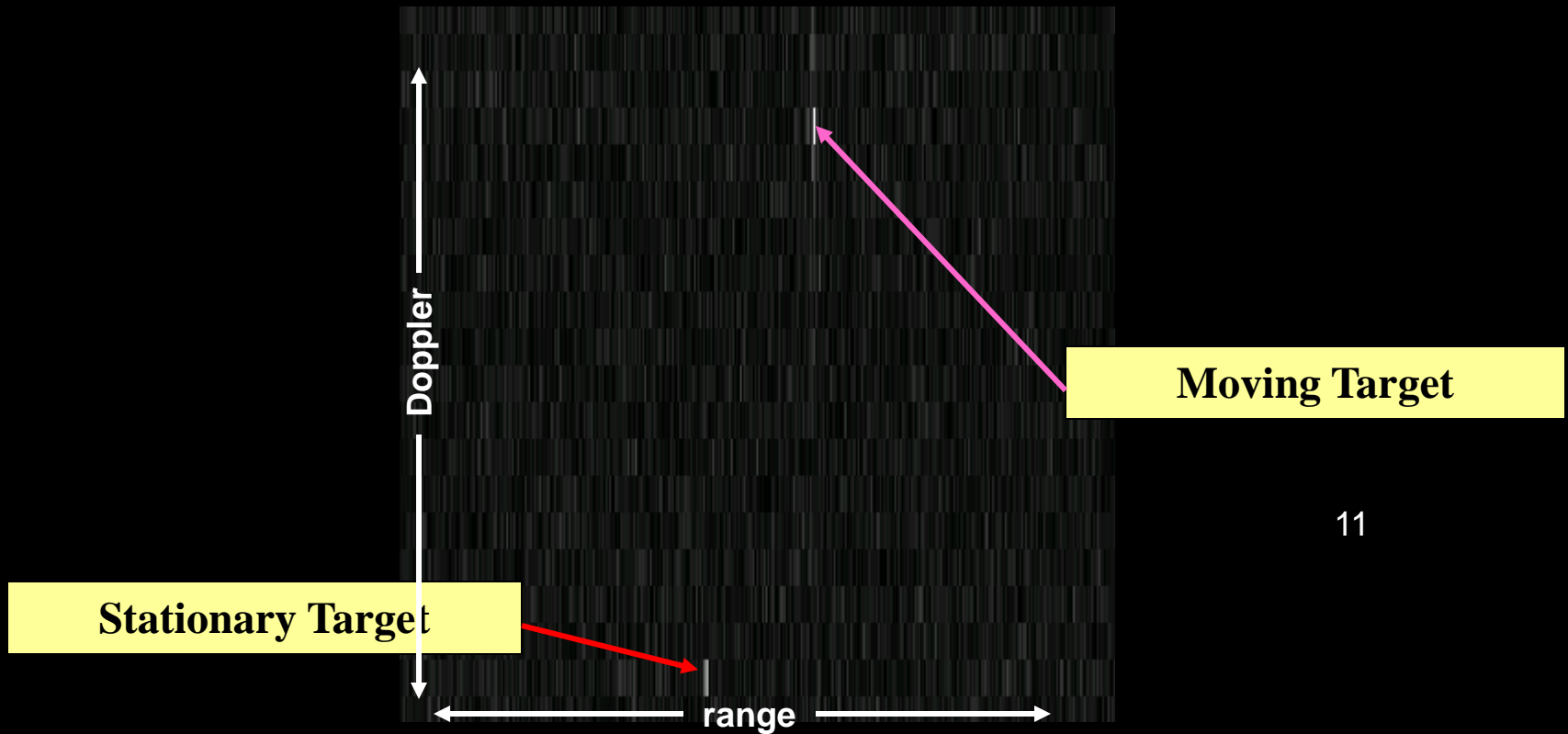
Moving Target Observed in Clutter Suppressed Imagery



10



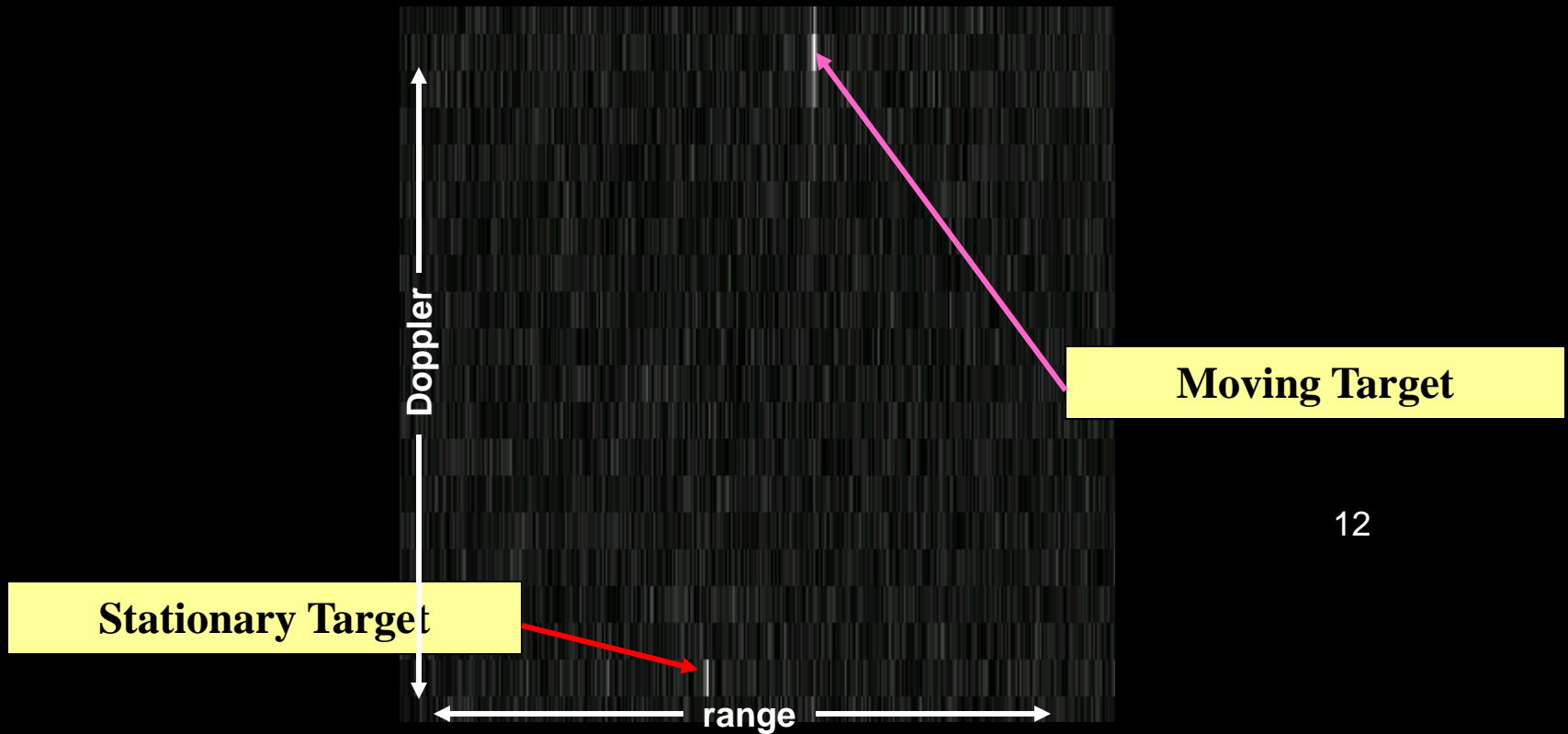
Moving Target Observed in Clutter Suppressed Imagery



11



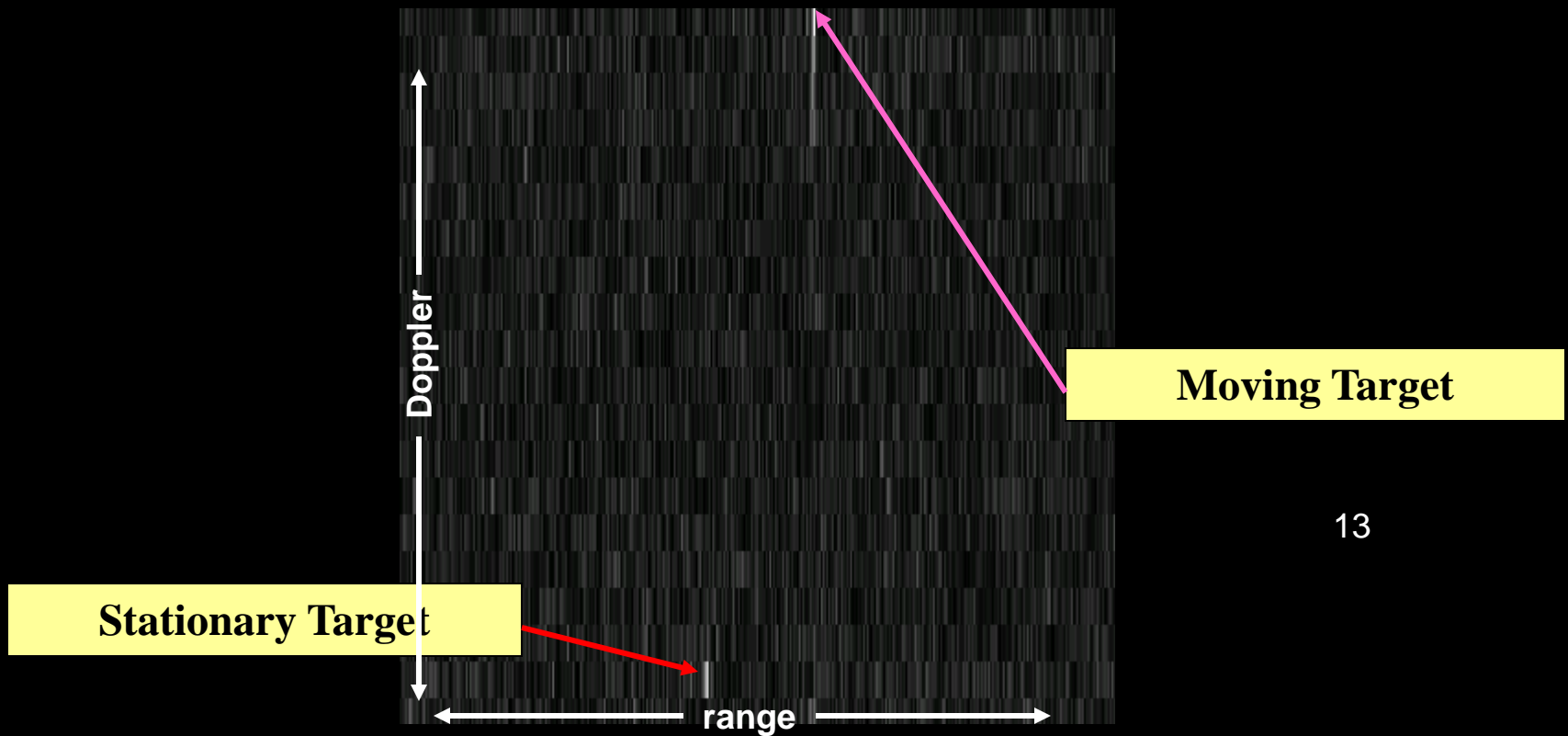
Moving Target Observed in Clutter Suppressed Imagery



12



Moving Target Observed in Clutter Suppressed Imagery



13



Ground Moving Targets in SAR Imagery

Summary

- Nominal Moving Target Phase Equations
 - Uncompensated motion leads to quadratic, cubic, .. phase
- Measured Moving Target Phase Examples
 - Cross range motion causes phase characteristics not displayed by stationary targets
- Space Time Adaptive Processing (STAP) Review
 - SINR, SINR loss, clutter suppression
- STAP applied to 8 channel SAR image data (element space, phase centers)
 - Single 2.7 sec coherent processing interval (CPI)
 - Thirteen, $2.7/13 = 0.2077$ sec. CPIs, results in SAR movie of moving vehicle, target migration through Doppler cells observed

Appreciation

- UCLA's Institute for Pure and Applied Mathematics
- Margaret Cheney
- The Aerospace Corporation



References

Rudge, A. W., Milne, K., Olver, A. D., Knight, P., The Handbook of Antenna Design, Vol. 1, Editors, copyright 1980.

Skolnik, M. I., Editor, Radar Handbook, McGraw-Hill Book Co., New York, ISBN 07-057908-3, Chap. 9 Aperture-antenna Analysis, by J. W. Sherman, pp 9-2 to 9-9, 1970.

Walker, J. L., "Range Doppler Imaging of Rotating Objects," IEEE Trans. Aerospace Electronic Systems, Vol. AES-16, pp. 23-52, Jan. 1980.

Brown, W. M., "Walker Model for Radar Sensing of Rigid Target Fields," IEEE Trans. Aerospace Electronic Systems, Vol. AES-16, pp. 104-107, Jan. 1980.

Munson, D. C., O'Brien, J. D., Jenkins, W. K., "A Tomographic Formulation of Spotlight-Mode Synthetic Aperture Radar," Proc. IEEE, Vol. 71, pp. 917-925, Aug. 1983.

Ausherman, D. A., et al, "Developments in Radar Imaging," IEEE Trans. Aerospace Electronic Systems, Vol. AES-20, No. 4, pp. 363-399, July 1984. This paper includes the Fourier transform result in the bistatic SAR case.

Jakowatz, C. V., Thompson, P. A., "A New Look at Spotlight-Mode Synthetic Aperture Radar as Tomography: Imaging Three-Dimensional Targets," IEEE Trans. Aerospace Electronic Systems, Vol. AES-4, No. 5, pp. 699-703, May 1995.

Carrara, W. G., Goodman, R. S., Majewski, R. M., Spotlight Synthetic Aperture Radar Signal Processing Algorithms, Artech House, Boston, ISBN 0-89006-728-7, pp. 501-506 (range deskew), 1995.

Jakowatz, C. V., Thompson, P. A., "A New Look at Spotlight-Mode Synthetic Aperture Radar as Tomography: Imaging Three-Dimensional Targets," IEEE Trans. Aerospace Electronic Systems, Vol. AES-4, No. 5, pp. 699-703, May 1995.

Jakowatz, C. V., Wahl, D. E., Eichel, P. H., Ghiglia, D. C., Thompson, P. A., Spotlight-Mode Synthetic Aperture Radar: A Signal Processing Approach, pp. 62-103, pp. 187-191, and Appendix C, Kluwer Academic Publishers, Boston, 1996.



References

Wehner, D. R., High Resolution Radar, Artech House, Boston, ISBN 0-89006-194-7, pp. 211-214, 1987.

Curlander, J. C., McDonough, R. N., Synthetic Aperture Radar Systems and Signal Processing, John Wiley & Sons, Inc., New York, ISBN 0-471-85770-X, pp. 120-124, 1991.

Brennan, L.E. Reed, I. S., Theory of Adaptive Radar, IEEE Trans. Aerospace and Electronic Systems, Vol. AES-9, No. 2, March 1973.

Ward, J., "Space-Time Adaptive Processing for Airborne Radar," MIT Lincoln Laboratory Technical Report 1015, December 13, 1994, Lexington, MA.

Guerci, J. R., Goldstein, J. S., Reed, I. S., "Optimal and Adaptive Reduced-Rank STAP," IEEE Transactions on Aerospace and Electronic Systems, Vol. 36, No. 2, pp. 647-663, April 2000.

Melvin, W. L., "A STAP Overview," IEEE A&E Systems Magazine, Vol. 19, No. 1, January 2004, Part 2: Tutorials-Melvin.

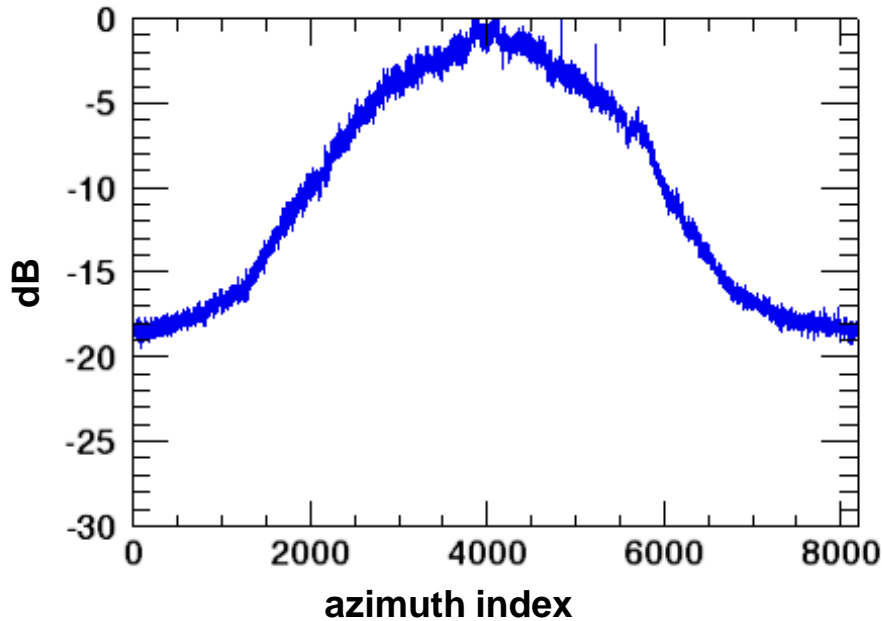


Backup Charts

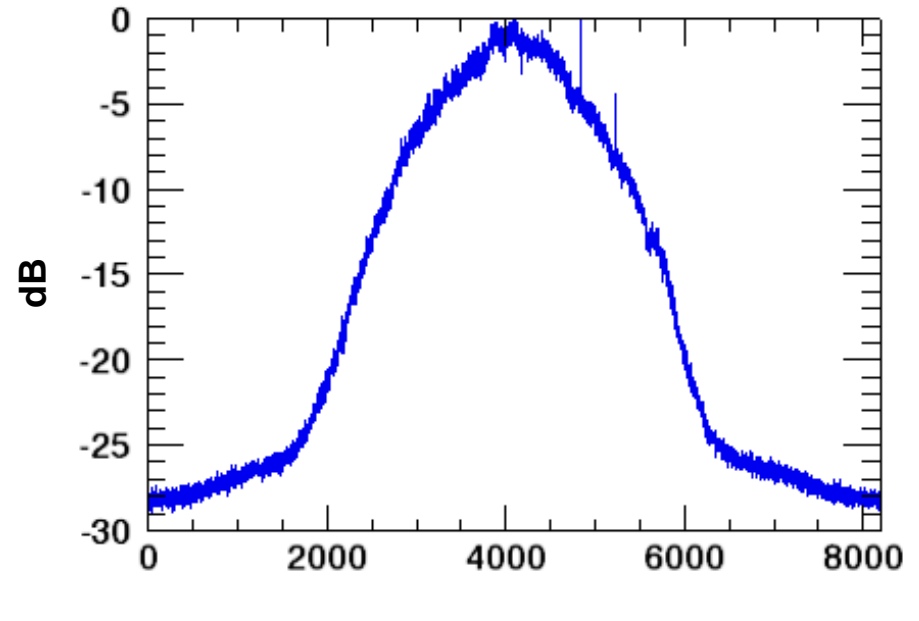


Antenna Patterns: Aircraft Data

Single element beam pattern



Beam pattern 8 element sum



PRF span

PRF span

Azimuth Beam pattern estimated using

$$b(y) = \sum_x |\sigma(x, y)|^2, \quad x = \text{range}, y = \text{azimuth}$$

$$B(y) = 10 \log_{10} (b(y)/b_{\max})$$

$b_{\max} = \max(b)$, max computed excluding large discretions

Observe: azimuth beamwidth narrows following summation of data from each azimuth element (channel)